UNCLASSIFIED

AD 274 228

Reproduced
by the

ARMED SERVICES TECHNICAL INFORMATION AGENCY
ARLINGTON HALL STATION
ARLINGTON 12, VIRGINIA

UNCLASSIFIED

NOTICE: When government or other drawings, specifications or other data are used for any purpose other than in connection with a definitely related government procurement operation, the U. S. Government thereby incurs no responsibility, nor any obligation whatsoever; and the fact that the Government may have formulated, furnished, or in any way supplied the said drawings, specifications, or other data is not to be regarded by implication or otherwise as in any manner licensing the holder or any other person or corporation, or conveying any rights or permission to manufacture, use or sell any patented invention that may in any way be related thereto.

274 228
CATALOGED BY ASTIA AS AD No. 274228

DASA REPORT NO. 1273

BRL

MEMORANDUM REPORT NO. 1390
MARCH 1962

INFORMATION SUMMARY OF BLAST PATTERNS IN TUNNELS AND CHAMBERS (Second Edition)

Shock Tube Facility Staff

N-62-3-1

Program was supported in part by the
Defense Atomic Support Agency; WEB No. 13.111

Ordnance Management Structure Code No. 5010.21.83024

BALLISTIC RESEARCH LABORATORIES

ABERDEEN PROVING GROUND, MARYLAND

B A L L I S T I C R E S E A R C H L A B O R A T O R I E S

MEMORANDUM REPORT NO. 1390

DASA REPORT NO. 1273

MARCH 1962

Information Summary of Blast Patterns in Tunnels and Chambers (Second Edition)

Shock Tube Facility
Terminal Ballistics Laboratory and Staff

Program was supported in part by the Defense Atomic Support Agency: WEB No. 13.111

Ordnance Management Structure Code No. 5010.21.83024
(Department of the Army Project No. 503-04-002
Ordnance Management Structure Code No. 5010.11.815)

A B E R D E E N P R O V I N G G R O U N D, M A R Y L A N D

PREFACE

The military requirements for protective construction have in recent years been most demanding since they include "blast hardened" designs. This in many cases means putting the construction deep underground and sets up requirements for information on the behavior of blast waves in confined region such as tunnels and chambers.

The Shock Tube Facility at the Ballistic Research Laboratories (BRL) endeavored to obtain information on the behavior of blast waves in tunnels and chambers by instrumenting models of simple tunnel configurations with piezo electric gages and subjecting the models to the blast wave from shock tubes. Data were obtained from models attached to the 24" circular tube, the 4" x 15" rectangular tube, and the high pressure tube. This report contains a compilation of the test results.

Work in this field is still in process at BRL and for that reason there will be supplements to this report. The more recent efforts are primarily directed toward establishing information for higher pressure regions.

TABLE OF CONTENTS

	PAGE
NOTATION	
1. INTRODUCTION	1-1
1.1 Objective	1-1
1.2 Layout of Report	1-2
1.3 Precautions	1-3
1.3.1 Limitations of Data	1-3
1.3.2 Wave Form	1-4
1.3.3 Wave Duration	1-6
1.3.4 Full Scale Verification	1-7
1.4 Conversion of Curves	1-8
2. BASIC BLAST PHENOMENA	2-1
2.1 The Shock Wave	2-2
2.2 Reflected Pressures	2-5
2.3 Stagnation Pressure	2-7
2.4 Drag Force	2-9
2.5 Sound Velocities Associated With Shock Waves	2-10
2.6 Velocity of a Reflected Wave	2-13
3. SHOCK ENTRY INTO TUNNELS	3-1
3.1 The Face-On Tunnel	3-1
3.1.1 Effect of the Reflecting Area	3-2
3.1.1.1 The Large Reflecting Area	3-2
3.1.1.2 Pressure in the Face-On Tunnel With a Large Reflecting Area	3-5
3.1.1.3 The Small Reflecting Area	3-7
3.1.2 Guide Lines for Predicting Pressures	3-9
3.2 The Side-On Tunnel	3-10
3.2.1 The Tunnel Side-On to a Shock Wave	3-10
3.2.2 Exceptions for the Side-On Tunnel	3-12

	PAGE
3.3 The Oblique Tunnel	3-14
4. TUNNEL JUNCTIONS	4-1
4.1 Side-On Tunnel Junctions	4-2
4.1.1 The Tunnel Side-On to an Equal Area Tunnel	4-2
4.1.2 The Tunnel Side-On to a Tunnel of Larger Area	4-4
4.2 The Pressure in the Primary Tunnel After a 90° Tunnel of Equal Area	4-5
4.3 The "T" Junction	4-7
4.4 The "Y" Junction	4-9
4.5 The "Cross" (+) Tunnel	4-11
5. THE ATTENUATION OF A SHOCK WAVE IN A TUNNEL	5-1
5.1 Predicting the Attenuation of a Shock Wave in a Tunnel	5-2
5.2 Predicting the Duration of a Shock Wave in a Tunnel	5-5
5.3 Determining the Attenuation in a Tunnel From a Nomogram	5-6
6. AREA CHANGES IN TUNNELS	6-1
6.1 Area Increases in Tunnels	6-2
7. SHOCK WAVE FILLING A CHAMBER THROUGH TUNNEL SYSTEMS	7-1
7.1 The Pressure-Time History in a Chamber	7-4
7.1.1 The Chamber Geometry	7-4
7.1.2 Construction of the Fill-Time Curve	7-5
7.2 Tunnel Configurations with Chambers	7-14
7.2.1 The Multiple Entrance	7-16
7.2.2 The Bypass Entrance	7-17
8. REFLECTED PRESSURES IN TUNNELS	8-1
8.1 The Short Tunnel	8-2
8.1.1 The Short Tunnel Side-On	8-3
8.1.2 The Short Tunnel Face-On	8-5
8.2 The Long Tunnel	8-6
8.3 Comparison of Reflected Pressures	8-8

PAGE

9. BLAST ARRIVAL TIMES IN TUNNELS 9-1

9.1 Shock Front Arrival Time 9-1

9.2 Time Interval Between Incident and Reflected Shock Waves in a Closed Tunnel 9-2

LIST OF FIGURES

		PAGE
Fig. 2.1	Shock Front Velocity and Particle Velocity as a Function of Shock Overpressure	2-3
Fig. 2.2	Reflected Shock Overpressure as a Function of Incident Shock Overpressure	2-6
Fig. 2.3	Incident Shock Overpressure vs. Stagnation Overpressure for a Standard Atmospheric Pressure of 14.7 Psi	2-8
Fig. 2.4	Sound Velocity Behind the Shock Front as a Function of the Shock Overpressure	2-11
Fig. 2.5	Sound Velocity Behind the Reflected Shock Front as a Function of the Reflected Shock Overpressure	2-12
Fig. 2.6	Velocity of the Reflected Shock Wave as a Function of the Incident Shock Overpressure	2-14
Fig. 3.1	Shock Formation Distance for Large Reflecting Area	3-3
Fig. 3.2	Incident vs. Transmitted Shock Overpressure for Face-On Tunnel	3-6
Fig. 3.3	Incident vs. Transmitted Shock Overpressure for a Face-On Tunnel with Various Baffle Tunnel Radii Ratio	3-8
Fig. 3.4	Incident vs. Transmitted Shock Overpressure for Side-On Tunnel	3-11
Fig. 3.5	Side-On Configurations with Reflected Pressures	3-13
Fig. 3.6	The Variation of Maximum Shock Overpressure in Tunnels with Angle of Incidence	3-15
Fig. 4.1	Incident vs. Transmitted Shock Overpressure for Tunnel Joined to an Equal Area Tunnel	4-3
Fig. 4.2	Incident Shock Overpressure vs. Shock Overpressure Transmitted Downstream of an Equal Area Tunnel Junction	4-6
Fig. 4.3	Incident Shock Overpressure vs. Transmitted Shock Overpressure for a "T" Tunnel Junction with Equal Area Tunnels	4-8
Fig. 4.4	Incident vs. Transmitted Shock Overpressure for a "Y" Tunnel Configuration	4-10
Fig. 4.5	Incident vs. Transmitted Shock Overpressure for a Cross, "+" Tunnel Configuration	4-12

		PAGE
Fig. 5.1	A Typical Pressure-Time Record of a Shock Wave with Tangent Drawn to Indicate the Time Intercept	5-3
Fig. 5.2	"K" as a Function of Shock Overpressure	5-4
Fig. 5.3	Nomogram for Determining the Attenuation of a Shock Wave Traveling in a Tunnel	5-7
Fig. 6.1	Incident vs Transmitted Shock Overpressure for a Tunnel Which Has an Area Increase	6-3
Fig. 7.1	Cyclic Nature of a Shock Wave in a Closed End Tunnel	7-2
Fig. 7.2	C vs Pressure Differential Between Applied Wave and Chamber	7-6
Fig. 7.3	Typical Tunnel Entrance and Chamber Configuration	7-7
Fig. 7.4	Applied Shock Wave	7-12
Fig. 7.5	Calculated Pressure-Time History in a Chamber	7-13
Fig. 7.6	Tunnel Chamber Configurations	7-15
Fig. 8.1	Short Tunnels Side-On and Face-On	8-4
Fig. 8.2	Maximum Reflected Shock Overpressure in Short Face-On Tunnels as a Function of Incident Shock Overpressures	8-7
Fig. 8.3	Reflected Shock Overpressures Developed in Tunnels for Three Entrance Conditions	8-9
Fig. 9.1	Time Interval Between Incident and Reflected Shocks as a Function of Distance and Pressure	9-3

NOTATION

a_1	Ambient sound velocity
a_2	Sound velocity behind the shock front
a_5	Sound velocity in the region of reflected shock pressure
A	Area (the cross-sectional area of a tunnel)
C	A function equal to (ft psi/sec) which will be defined further in Section 7.1.2
D	Diameter (the diameter of a tunnel)
h	Height
K	A function necessary in the calculation of the attenuation in a tunnel which will be defined further in Section 5.1
P_s	Incident shock overpressure
P'_s	Shock overpressure after interaction
P_{stag}	Stagnation overpressure
P_t	Shock overpressure at time t
P_{s_x}	Shock overpressure in a tunnel after a travel of x distance
P_1	Atmospheric pressure
P_4	Overpressure in a chamber
P_5	Reflected shock overpressure
P_{21}	Absolute shock ratio
r	Radius of a tunnel
R	Radius of a reflecting area around a tunnel entrance
S	Perimeter of a cross section of a tunnel
t	Time
u	Particle velocity behind a shock wave

U	Shock front velocity
U_5	Velocity of reflected shock wave
V	Volume (the colume of a chamber)
x	Distance along a tunnel
α	Angle of incidence
θ	A constant used in calculation of attenuation equal to 0.13 sec/ft
τ_o	Total positive phase duration of the shock wave
τ	Time intercept of the incident wave
τ'	Effective time intercept presented to the remainder of a tunnel at a junction
τ''	Effective time intercept presented to the side-on tunnel at a junction

1. INTRODUCTION

1.1 Objective

The information contained in this publication is assembled to provide designers of protective construction with information that will aid them in determining the pressures which may be expected in tunnels and tunnel systems as a result of a bomb burst exterior to the tunnel.

1.2 Layout of Report

This report is presented in a manner conducive to immediate use by the design engineer. The curves in the body of the report are presented in terms of overpressure based upon an assumed atmospheric pressure of 14.7 psi. A section of this chapter discusses the method to be used in converting the curves to pressure ratios so that the information presented can be applied where the atmospheric pressure is other than 14.7 psi. Section 2 of this report deals with basic blast phenomena and contains sufficient information for a proper interpretation of the material in the report.

1.3 Precautions

1.3.1 Limitations of Data

The majority of curves in this report are based on experiments conducted at the BRL Shock Tube Facility. In some cases, where a need for information exists and the experimental work has not begun, theoretical curves are presented. In most cases supplements to this report will show data to substantiate curves based on theoretical considerations.

As stated earlier, data were obtained using the family of shock tubes at the BRL and this of course means that all data were obtained on models. There is no evidence to cast any doubt about using these data for prototype conditions, in fact, there is some to support it, (See Section 1.3.4).

The curves presented show input pressures between 10 and 1000 psi. For the input pressures above 35 psi data were obtained on either the high pressure shock tube or the 4 x 15" shock tube. On the latter the expansion chamber was evacuated and data obtained from equivalent shock strengths.

The curves drawn through the experimental data were constructed merely to show the trend of the data and for that reason may be extrapolated to some degree. The reader is urged to consider the scatter in the data points when making a reading from the curve.

1.3.2 Wave Form

Effective application of the methods presented in this report depend greatly upon the accuracy to which the assumed upper limits of pressure and wave duration fit the true expected wave form. This then necessarily leads to a requirement for target analysis based on probable bomb yield, ground range, height of burst, orientation and ground surface condition.

In this report it is assumed that only the applied free stream pressure, wave form and flow direction in the immediate vicinity of the target is given. It is also assumed that the shock is free from any loading of foreign matter and that the shock is classical in nature. The discussions contained herein will apply mainly to shock waves that are free from any anomalies which might arise from intense pre-shock thermal radiation.

Such restrictions must be placed on the use of this data because the data were obtained under classical shock condition. However, there are other factors and bits of information which when considered as a whole, make the anomalous wave shape not quite so undesirable.

For instance, shock tube experiments show that a compressional wave tends to become a shock when the driving force is sustaining. This means that only the entrance conditions (Chapter 3) would be effected by a precursor type wave, since once the wave is in the tunnel and has traveled some distance it will shock-up. Outside of the tunnel complex the non-ideal wave form is a very good possibility. It should work to the designers advantage for side-on orientations because

higher speed flows over the tunnel entrance have a greater resistance to turning. In the face-on case it will be a disadvantage in that one may expect higher pressures initially in the tunnel. Figure 3.2 has a dashed-in curve which may be used for predicting pressures when precursors are expected.

1.3.3 Wave Duration

The durations of the shock waves used to obtain the experimental data presented were in all cases very long and exhibited a step (or constant pressure) wave form for a time in excess of the times required for a shock wave to undergo the changes that were measured. This constant pressure shock wave is equivalent to an infinitely long shock wave and hence will give an overestimate of the true pressure when compared to a classical shock wave. The classical blast wave will, for the purposes of selecting a standard for this report, decay with time according to Friedlanders equation which is expressed as;

$$P_t = P_s \left(1 - \frac{t}{\tau_o}\right) e^{-t/\tau_o} \quad .$$

This means that at any given time during the passage of the shock wave the pressure will be less than the step shock wave. For very high pressures the above equation is not a good approximation because the decay rate is quite high. As stated earlier these factors produce errors in predicted pressures but they favor the designer since they indicate higher pressures than will be realized. The relationship $\tau_o > \frac{50\ D}{a_1}$ may be used as a guide line for determining when these data may be used without introducing an error of greater than 5 per cent. This will apply when the Friedlanders curve approximately fits the predicted wave form.

1.3.4 Full Scale Verification

The paucity of full scale data makes it impossible to state with certitude, that all the scale model data presented here can be substantiated by a full scale test. Test data are presented on tunnel sizes from 7/8" to 22 1/2" but the large gap from these, to dimensions of the order of 20 feet may cause some concern. It should be stated here, that there is no reason to believe that a large change in the scale factor will effect the data presented, however efforts are being made to conduct tests on much larger models, so that a measure of certainty can be obtained.

On a recent field test, a 4 ft. diameter tunnel was exposed to the blast from 100 tons of TNT. The measured data substantiates, in part, the tunnel attenuation data presented in Chapter 5.

1.4 Conversion of Curves

Throughout the body of this report the curves are plotted as a function of shock overpressure based on the standard atmospheric pressure of 14.7 psi. In some instances where it is desirable to apply these curves to experiments or to design for construction under extreme conditions or high altitudes, it will be beneficial to convert these shock overpressures to absolute shock ratios where ambient pressure is taken into consideration.

It is suggested that for atmospheric pressures of 13 psi and below, the shock overpressures presented herein be converted to absolute pressure ratios for comparison to local conditions. Absolute shock ratio is defined as being $(P_s + P_1)/P_1$. The symbol commonly used to designate the absolute pressure ratio across the shock front is P_{21}.

In order to convert the pressure axis of the curves presented in this report to P_{21}, the individual values of overpressure, from the pressure axis, should be added to the standard atmospheric pressure of 14.7 psi and these values should be divided by the same atmospheric pressure of 14.7 psi. These values should then replace the values of shock overpressure now found on the curves. It should be noted that for a shock overpressure of zero, P_{21}, will have the value 1, and that all absolute shock ratios will be greater than 1.

Since it is decidedly easier for the individual to think in pounds per square inch of overpressure than in absolute pressure ratio, it is felt that for ease of understanding, the conversions to absolute pressure ratio should be performed only for those conditions previously mentioned.

2. BASIC BLAST PHENOMENA

The interpretation of the material within this report requires some knowledge of the basic blast phenomena and this chapter is designed to satisfy that requirement. The reader is referred to the "Effects of Nuclear Weapons"* for a comprehensive treatment of the phenomena.

* "The Effects of Nuclear Weapons", Washington 25, D. C. : Department of the Army Pamphlet No. 39-3, May 1, 1957.

2.1 The Shock Wave

The violent release of thermal energy in a gaseous medium gives rise to a sudden pressure increase in that medium. This pressure disturbance, termed the shock wave, is the rise from the ambient pressure to the peak value in a time of the order of 10^{-8} seconds. This pressure jump or shock front travels radially from the burst point, with a diminishing velocity which at all times is in excess of the sonic velocity in the medium through which the shock is travelling. The gas molecules making up the wave move at velocities less than that of the shock front. Both of these velocities, that of the front and that of the gas, are functions of the magnitude of the pressure. Curves showing the relationship between shock front pressure, the velocity of the shock front, and particle velocity are shown in Figure 2.1. The relationships shown in Figure 2.1 are independent of the magnitude of the explosion, however, the distance from the explosion at which any pressure or velocity is obtained is a definite function of the magnitude of the explosion. The magnitude of the explosion governs the time interval between the initial pressure jump and the return of pressure to atmospheric pressure. This interval is termed the positive phase duration and is generally referred to as "duration". The larger the explosion, the greater the duration and hence the greater will be the distance that the shock wave will travel.

The positive phase of the wave is followed by the negative phase which is approximately 5 times the duration of the positive phase. The negative phase is characterized by a pressure below the pre-shot atmospheric pressure and a reversal of the particle flow. This is a relatively unimportant phase of the blast wave.

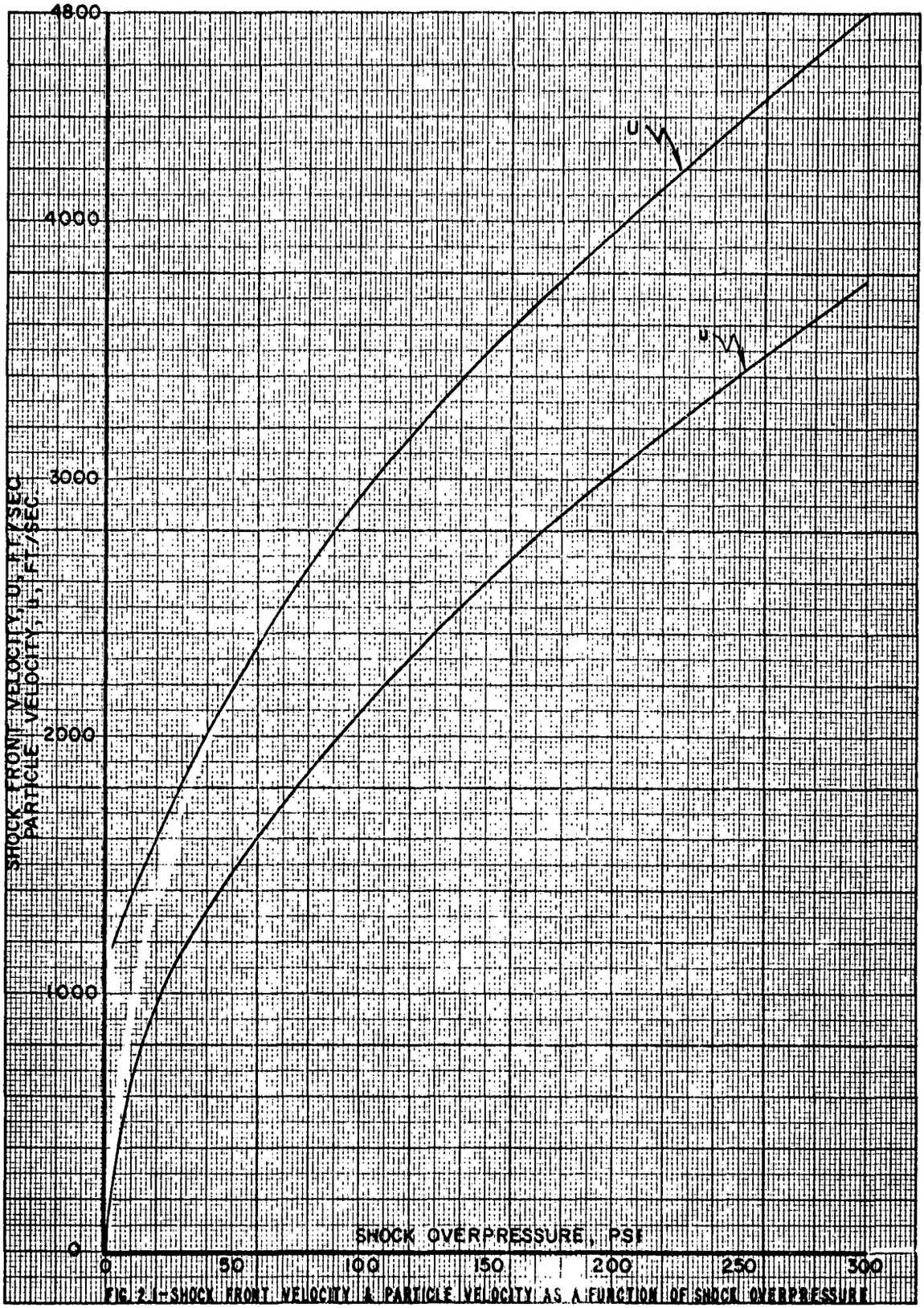

FIG 2.1-SHOCK FRONT VELOCITY & PARTICLE VELOCITY AS A FUNCTION OF SHOCK OVERPRESSURE

A shock wave is normally identified by its peak pressure and duration. The term peak pressure is used synonymously with, incident pressure, side-on pressure, or shock overpressure and it refers to the static component of the blast wave. Since the blast wave is moving any attempt to measure the side-on component is complicated by dynamic effects. A pressure sensing device positioned side-on to the wave will, for all practical purposes measure the side-on component, however, a sensor at angles to the wave will receive some pressure component resulting from the motion of the pressure field in addition to the side-on component. When the shock wave path is altered by some rigid obstruction, the shock wave is diffracted about the obstruction. The pattern of such a diffraction consists of reflection, stagnation, rarefaction, and compression waves.

2.2 Reflected Pressures

When a shock wave impinges on a rigid surface oriented 90 degrees to the direction of propagation of the wave, a reflected pressure is instantly developed on the surface. The magnitude of reflected pressure is about twice the incident pressure for weak shocks and approaches a factor of greater than 8 times the applied pressure for very strong shocks. Figure 2.2 shows the relationship between reflected and incident pressures. The reflected pressure is important because of its magnitude and rate of application.

In a closed tunnel system the shock wave that reflects from the blind end of a tunnel must pass back through itself. Its duration then will be a direct function of the duration of the incident wave. In an open system, one which permits flow around the edge or edges of a reflector, the duration of the reflected pressure is controlled by the size of the reflecting surface, provided of course, that the duration of the wave is long. The high reflected pressure seeks relief towards the lower pressure region. This tendency for equalization is satisfied by the propagation of rarefaction waves from the low pressure regions to the high pressure region. These rarefaction waves travel at the velocity of sound in the medium. The duration of the reflected pressure will be quite small on small targets even though the total wave duration may be long. Reflected pressure is thereby reduced to the stagnation pressure by the action of the rarefaction wave.

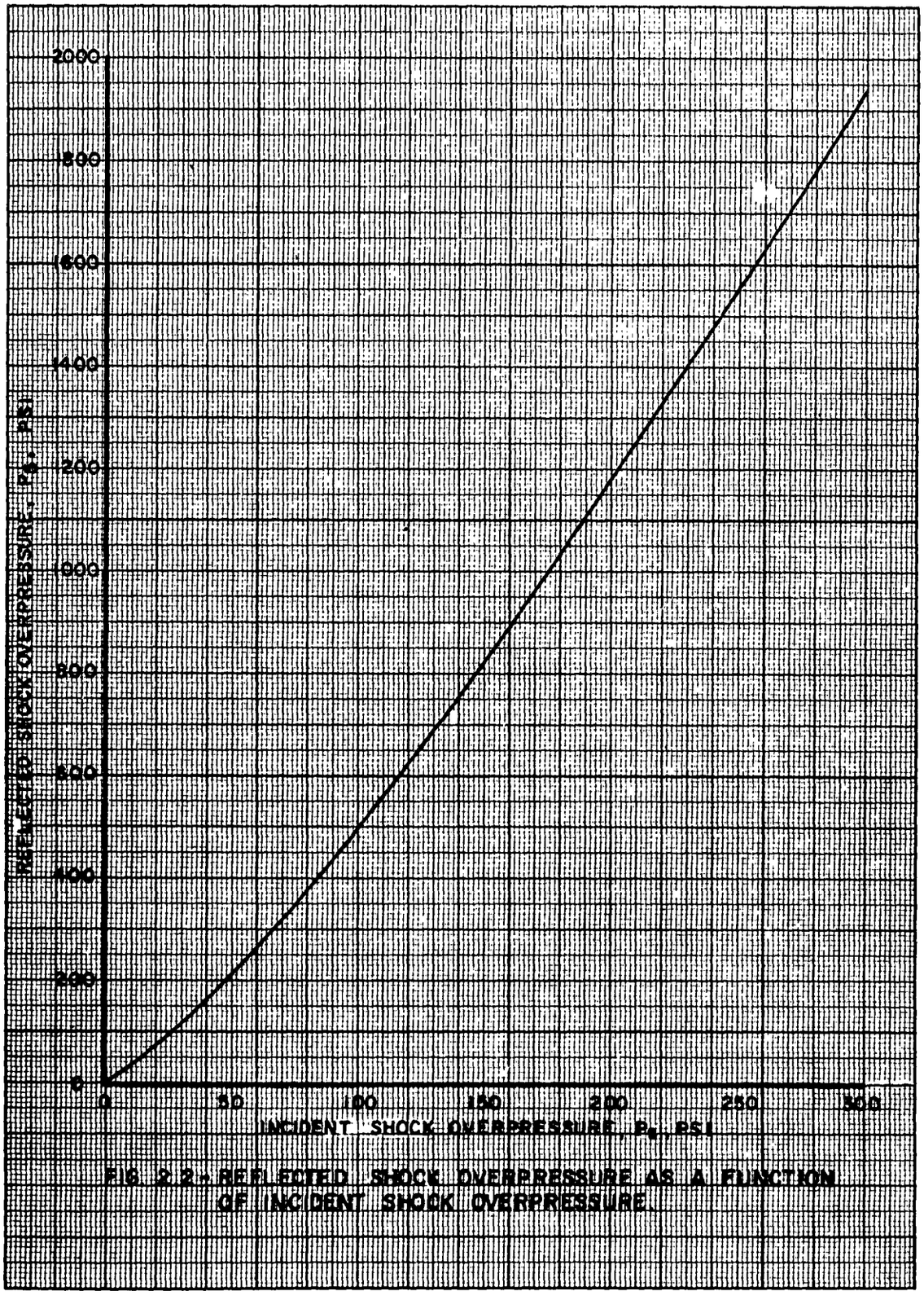

FIG. 2.2 - REFLECTED SHOCK OVERPRESSURE AS A FUNCTION OF INCIDENT SHOCK OVERPRESSURE.

2.3 Stagnation Pressure

Once the shock wave has encountered the normal reflecting surface, and the reflected wave has been relieved, stagnation pressure exhibits itself on the reflecting surface. This pressure is a result of the air particles coming to rest on the reflecting surface and transforming the dynamic momentum of air particles to static pressure. The resulting pressure region will be sustained as long as there is flow and its magnitude will be a function of the flow velocity and density. A curve showing incident shock overpressure versus stagnation overpressure is shown in Figure 2.3. It can be shown then that by far the majority of impulse delivered to a small target by a long duration wave is contributed by stagnation pressure. It should be noted here that while stagnation pressure may be exerted on the reflecting surface of an object, the rear surface (back side of a wall) has a distinctly lower and different pressure pattern. The net force on the reflector will be the difference between the face-on and rear-on forces. This difference is often called the drag force.

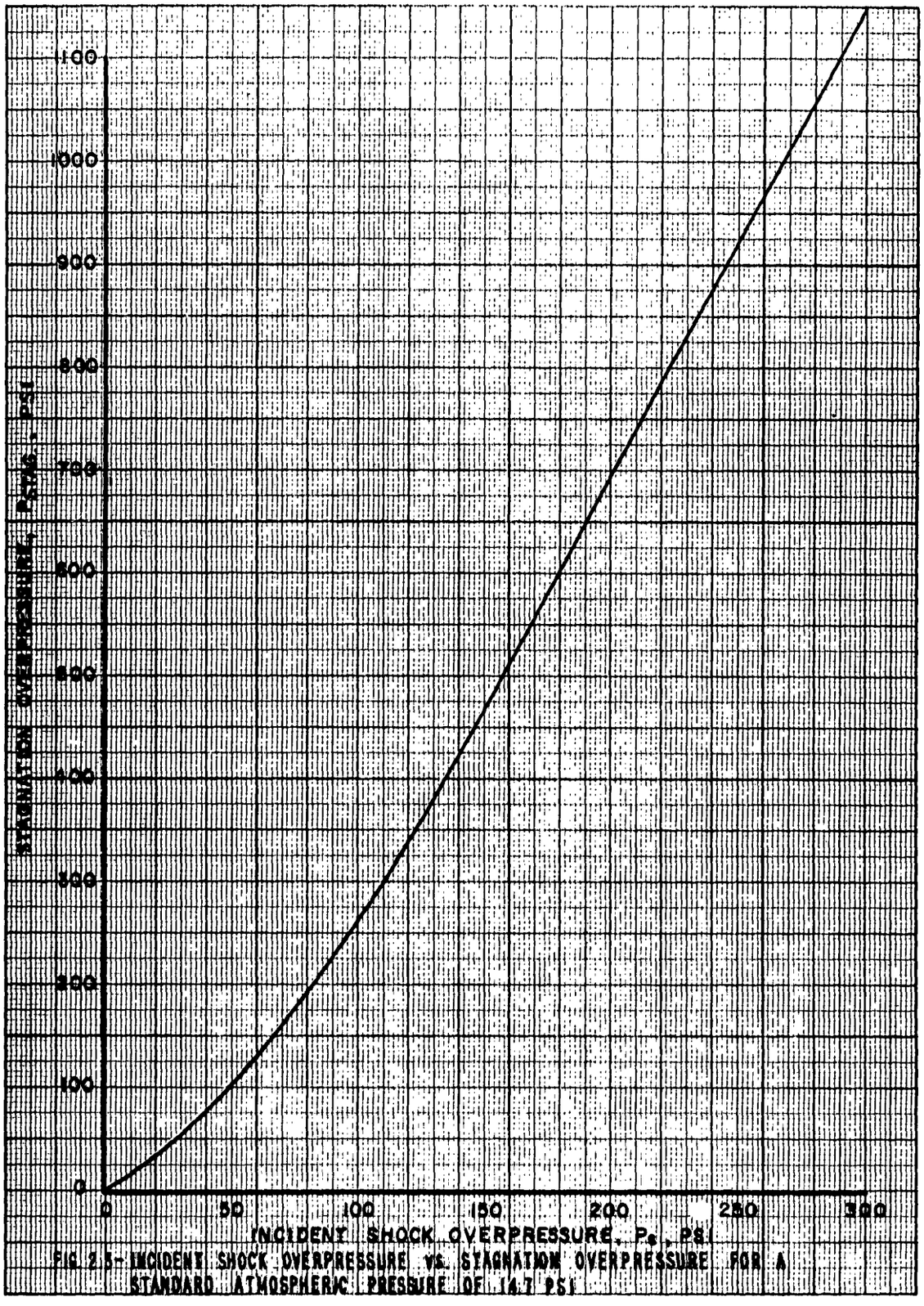

FIG. 2.5 - INCIDENT SHOCK OVERPRESSURE vs. STAGNATION OVERPRESSURE FOR A STANDARD ATMOSPHERIC PRESSURE OF 14.7 PSI

2.4 Drag Force

The drag force can be defined as that force which tends to translate an object immersed in the air stream of a shock wave. This is actually the vector sum of the two forces; the tangential force resulting from the surface friction and the normal or pressure force. For the purposes of this report the latter is of primary concern and can be considered the resultant force between the front and rear surfaces of the target. The governing parameters for the drag force are the velocity of the air particles, the density of the air stream, and the shape of the target. One can roughly approximate the drag force by neglecting the shape of the object and taking the difference between the force on the front which results from stagnation pressure and that on the rear, which is assumed to be side-on pressure.

When the shape of an object is neglected, one assumes a drag coefficient of 1. This coefficient is a number which relates the shape of an object to the flow field in which it is immersed. It is obvious that in streamlining a target the pressure distribution about the target is greatly altered and hence causes two objects with the same frontal areas to exhibit different resistant forces.

2.5 Sound Velocities Associated With Shock Waves

As stated earlier the curves in this report are plotted as a function of shock overpressure based on an atmospheric pressure of 14.7 psi. It was also necessary to assume a sound velocity in the medium through which the shock is traveling since this parameter also effects the shock wave behavior. The curves in this report are based on a sound velocity of 1117 ft/sec.

In order to perform certain of the manipulations of shock waves presented in later sections of the report, it will be necessary to be aware of the sound velocities associated with various parts of the shock wave. Figure 2.4 and 2.5 are plots of the sound velocity behind the shock front and sound velocity behind the reflected shock front as a function of shock overpressure and reflected shock overpressure respectively.

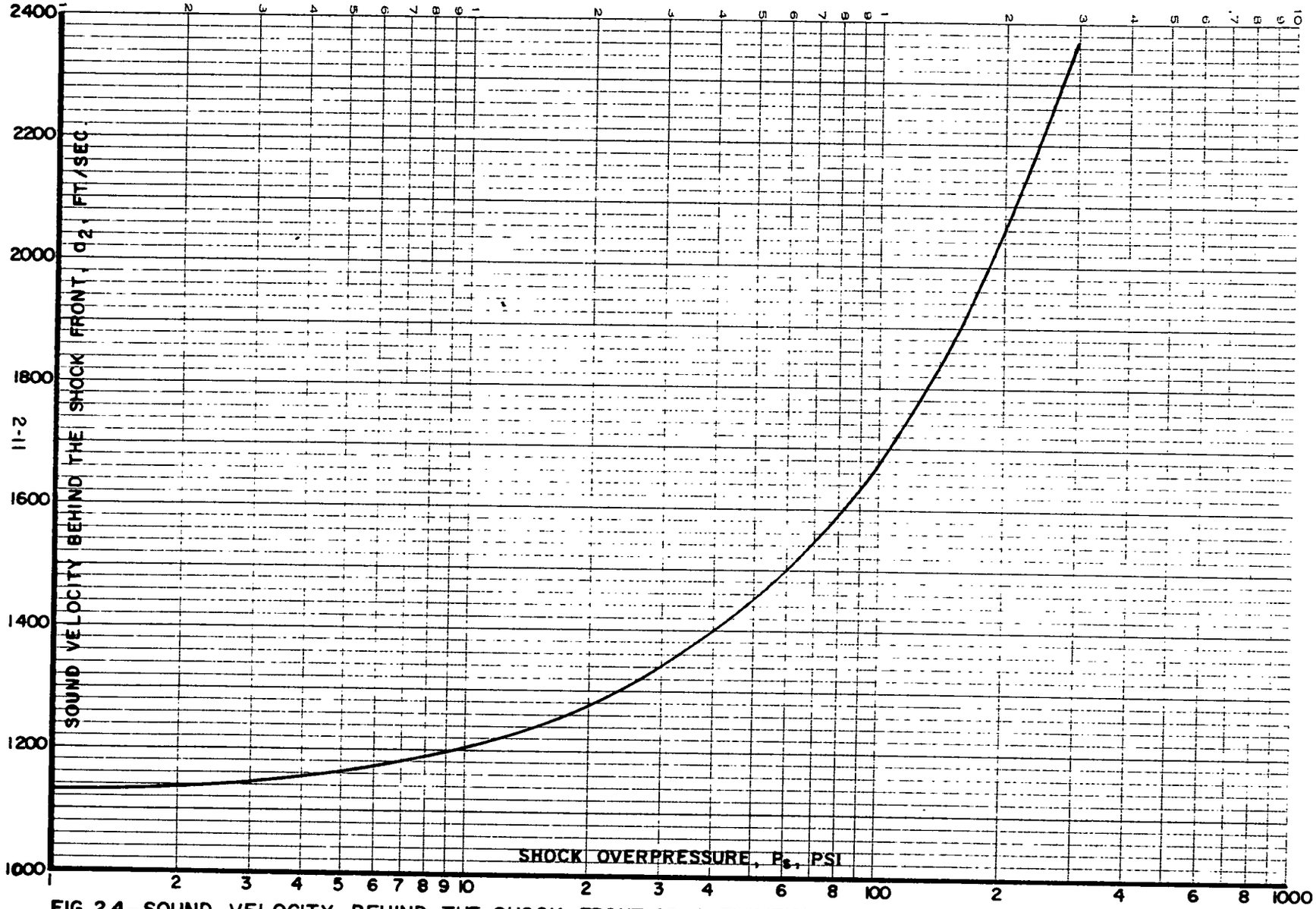

FIG. 2.4 – SOUND VELOCITY BEHIND THE SHOCK FRONT AS A FUNCTION OF THE SHOCK OVERPRESSURE

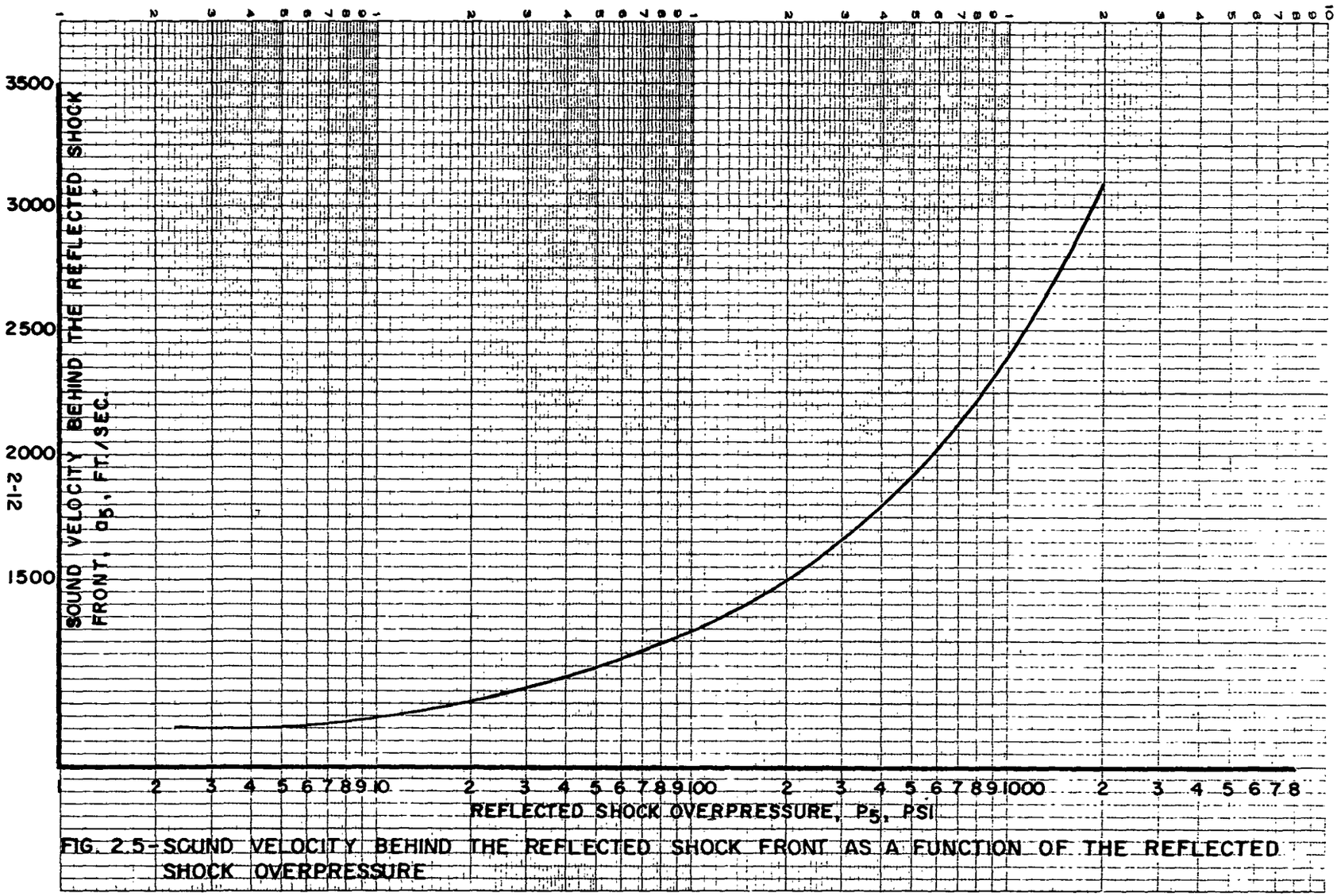

FIG. 2.5 - SOUND VELOCITY BEHIND THE REFLECTED SHOCK FRONT AS A FUNCTION OF THE REFLECTED SHOCK OVERPRESSURE

2.6 Velocity of a Reflected Wave

When a shock wave reflects and passes back through itself the pressure of the reflected wave is as shown in Figure 2.2. The velocity of this reflected wave is plotted in Figure 2.6 as a function of the incident wave.

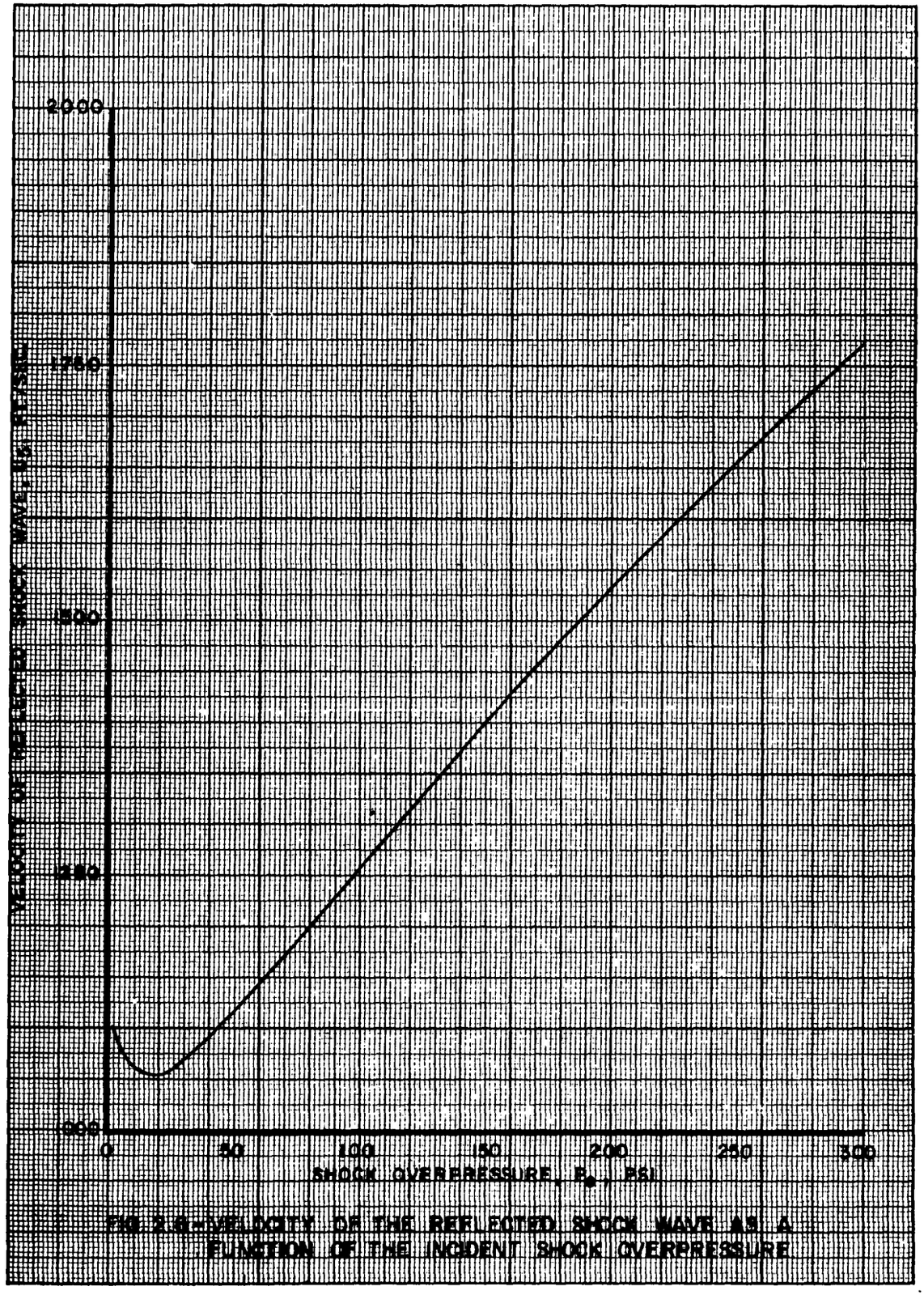

FIG 2.6—VELOCITY OF THE REFLECTED SHOCK WAVE AS A FUNCTION OF THE INCIDENT SHOCK OVERPRESSURE

3. SHOCK ENTRY INTO TUNNELS

3.1 The Face-On Tunnel

The orientation of a tunnel entrance plays a major part in determining the strength of a shock wave that is propagated through the tunnel. Also the geometry of the area in the vicinity of entrance influences the shock transmitted into the tunnel. For instance, for the face-on case, if a tunnel has a large reflecting area surrounding it such as a tunnel in the face of a large sheer cliff, a long duration reflected pressure will exist on the surface in the region of the tunnel entrance when a shock wave is incident upon the cliff. This reflected pressure region enhances the shock wave that is propagated into the tunnel. On the other hand a thin wall pipe with its entrance facing the blast would merely confine the shock wave to a one dimensional expansion after it enters the tunnel. The pressures transmitted in a tunnel for the two extremes in entrance condition are quite different.

3.1.1 Effect of the Reflecting Area

3.1.1.1 The Large Reflecting Area

When a shock wave impinges on a tunnel surrounded by a large reflecting area, the new shock formed in the tunnel is stronger than the applied incident wave. Some time is required to form the new shock to this increased value and this time is a function of the diameter of the tunnel, the incident shock pressure, and the area of the reflecting surface. The area of the reflecting surface and the diameter of the tunnel are the determinates for the thickness of the reflected pressure region. A large ratio of reflecting area to tunnel area will produce a reflected pressure region sufficient in size to permit the shock to form without noticeably affecting the reflected pressure zone.

When the reflecting area is not large enough to sustain the reflected pressure until the new shock wave is fully developed in the tunnel, the formation distance will be shorter, yielding pressures less than those resulting from the larger reflecting area. When the reflecting surface is limited in extent, a rarefaction from the outer edge of the surface will reduce the reflected pressure and the maximum possible transmitted pressure.

Figure 3.1 shows a reflecting surface, tunnel combination where the reflecting surface is considered large. The tunnel is instrumented with pressure-time gages. The gage position close to the entrance indicates the incident pressure of the applied peak pressure wave and as the wave progresses down the tunnel the peak pressure increases. It maximizes at a distance of about 10 diameters and then begins to decay. Pressure-time curves at the positions close to the orifice show a complex wave form that comprises both the incident wave form and some of the higher pressure of the reflected zone. The distance

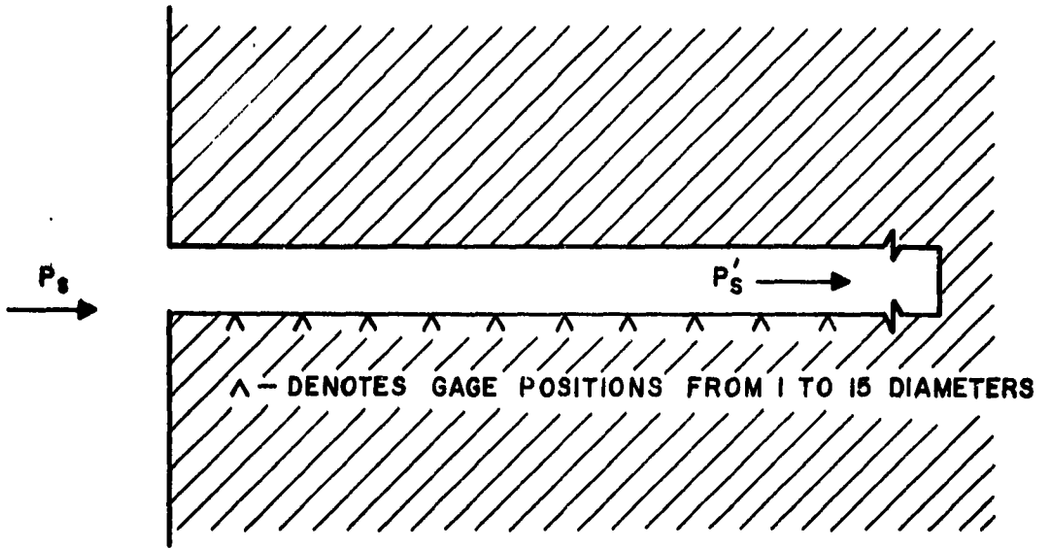

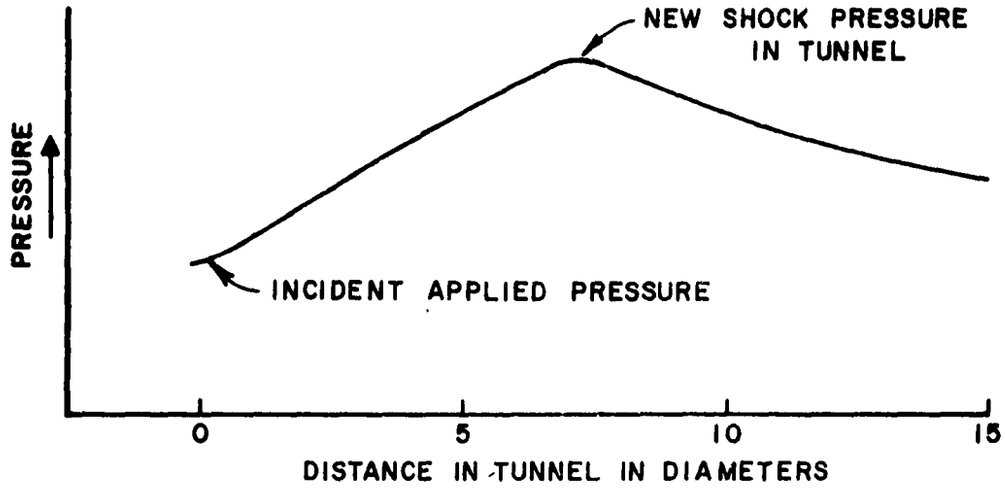

FIG. 3.1
SHOCK FORMATION DISTANCE FOR LARGE REFLECTING AREA

required for these two pressures to coalesce and form the maximum shock is considered the formation distance. BRL experiments to date indicate this distance to be between 5 and 10 diameters. For the purpose of establishing continuity of design criteria it is suggested that the assumption be made that the pressure in a tunnel will maximize at a distance of 10 tunnel diameters from the entrance or other disturbing condition. This factor should be considered when designing tunnels.

3.1.1.2 Pressure in the Face-On Tunnel With a Large Reflecting Area

When a shock wave is face-on to a large plane surface of a tunnel entrance, the newly formed wave enters the tunnel and builds to the maximum pressure in 10 diameters down the tunnel. A curve showing this maximum pressure as a function of the incident pressure can be found in Figure 3.2.

In the event that an anomalous wave shape is predicted for the face-on condition it is suggested that the dashed curve in Figure 3.2 be used to predict the pressures in the tunnel.

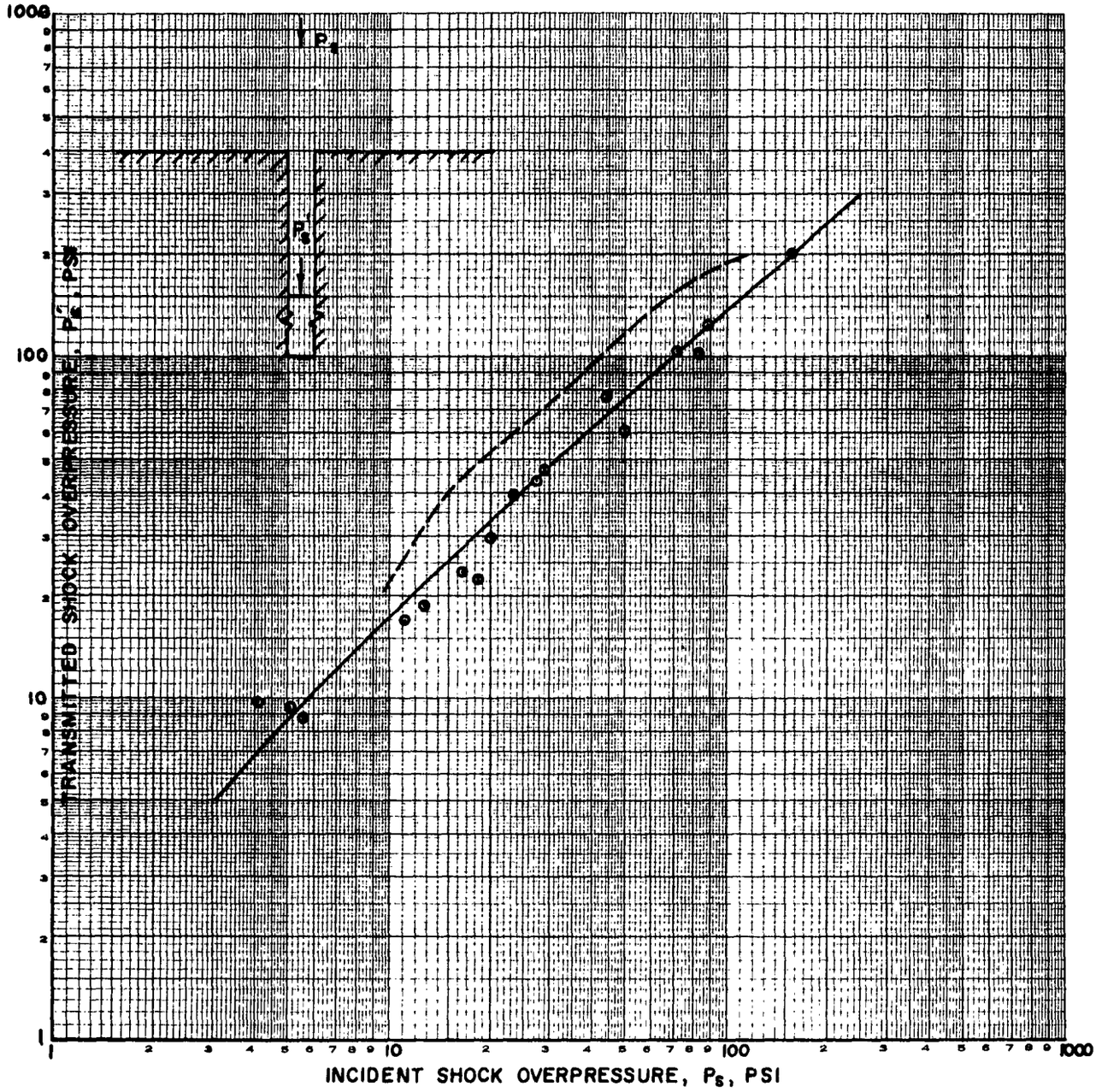

FIG. 3.2 – INCIDENT vs. TRANSMITTED SHOCK OVERPRESSURE FOR FACE-ON TUNNEL.

3.1.1.3 The Small Reflecting Area

When a reflecting area (baffle) is not large enough to sustain the reflected pressure until the new shock wave is fully developed in the tunnel, the shock formation distance will be shorter, yielding pressures less than those resulting from a large reflecting area. When the reflecting surface is so limited, a rarefaction from the outer edge of the surface will reduce the reservoir of reflected pressure to the extent that the maximum possible transmitted pressure will not be achieved.

Figure 3.3 shows curves which may be used to predict the maximum shock pressure developed in a tunnel for several baffle-tunnel radii ratios. It should be noted here that for a baffle-tunnel radii ratio of one, that pressure transmitted into the tunnel will be the same as the incident shock wave since no baffle or reflecting area exists to cause wave interaction. It might also be mentioned that for an infinite baffle-tunnel radii ratio, Figure 3.2 will be applied as the upper limit of Figure 3.3.

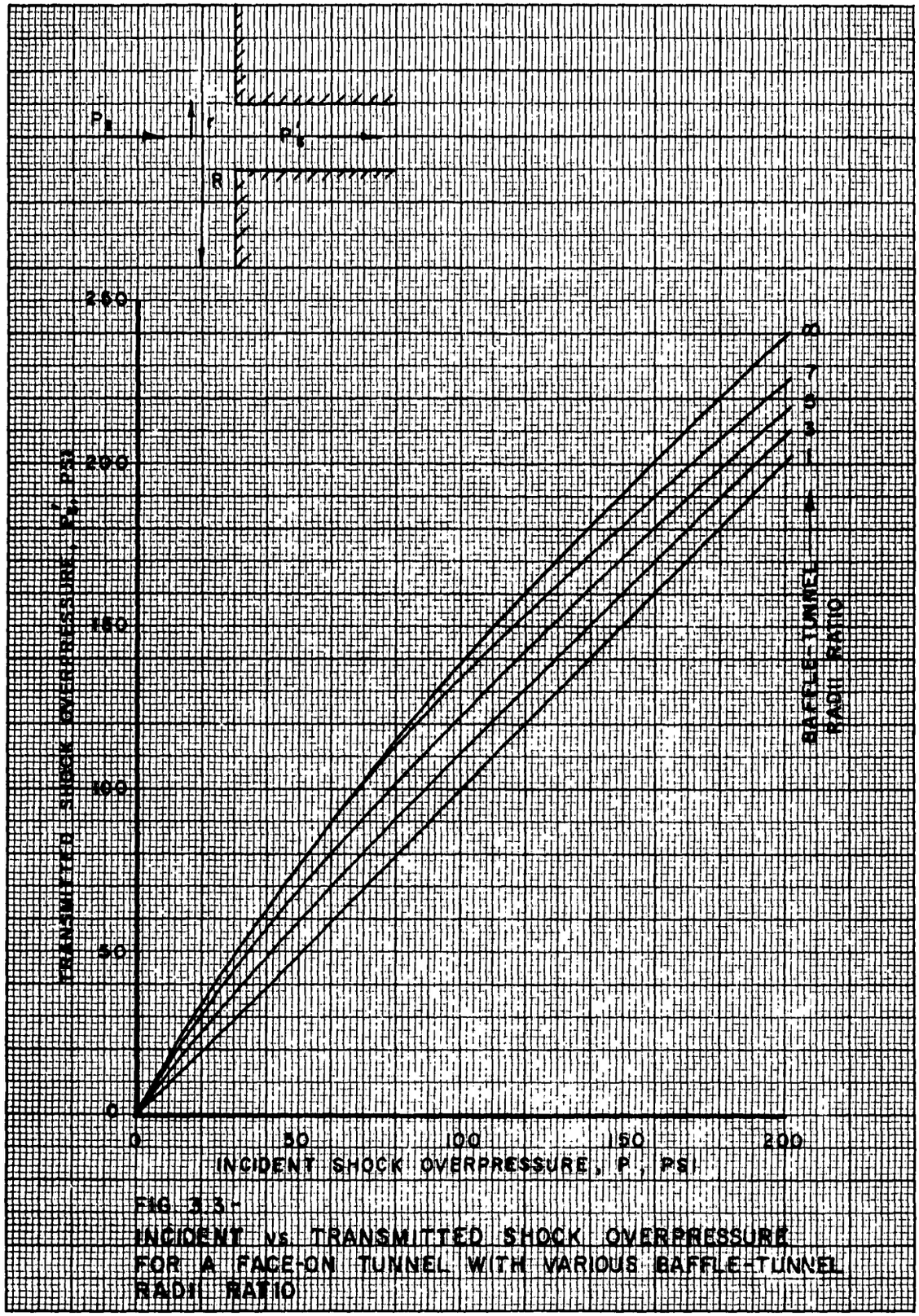

FIG. 3.3 -
INCIDENT vs. TRANSMITTED SHOCK OVERPRESSURE FOR A FACE-ON TUNNEL WITH VARIOUS BAFFLE-TUNNEL RADII RATIO

3.1.2 Guide Lines for Predicting Pressures

Guide lines for the valid use of the curve in Figure 3.2 are set out as follows:

a. The distance between the periphery of the tunnel and the edge of the reflecting surface should be at least two tunnel diameters. If the tunnel is not in the center of the reflecting surface, then the distance to the nearest relieving edge will determine the relief time of the reflected pressure and the resulting maximum tunnel pressure.

b. Any rigid surface capable of withstanding the reflected pressure can be considered a reflecting surface, and unless the surface has a roughness with perturbations comparable in size to the tunnel diameter, it can be considered smooth.

c. The conditions for input wave duration as outlined in Section 1.3.3 should be adhered to. An approximate figure for valid use of the curve however, is a duration where $\tau_o > \frac{50\ D}{a_1}$. If the duration of the applied wave is less than $\frac{50\ D}{a_1}$ then pressures less than those predicted from Figure 3.2 will be obtained.

3.2 The Side-On Tunnel

3.2.1 The Tunnel Side-On to a Shock Wave

When a shock wave approaches a tunnel so that the tunnel axis is 90 degrees to the direction of travel of the applied shock, the shock wave propagated in the tunnel will be less than the incident shock wave. The driving pressure here for the new shock wave is the incident pressure of the applied shock.

A verticle shaft in the earth, over which the shock wave travels, has a very large shocked air volume on the surface of the ground to drive the new shock and the shock in the tunnel will maximize as a result of this. The curve in Figure 3.4 will enable one to predict the new shock pressure in the side-on tunnel when the applied shock pressure is known.

It might also be pointed out that the case of a tunnel side-on to a second tunnel, where the first tunnel is very large compared to the one in question, may be considered as being a tunnel side-on to a shock wave traveling along the surface of the ground. In this case also, the pressure transmitted into the tunnel may be found from Figure 3.4 when the pressure in the large tunnel is known.

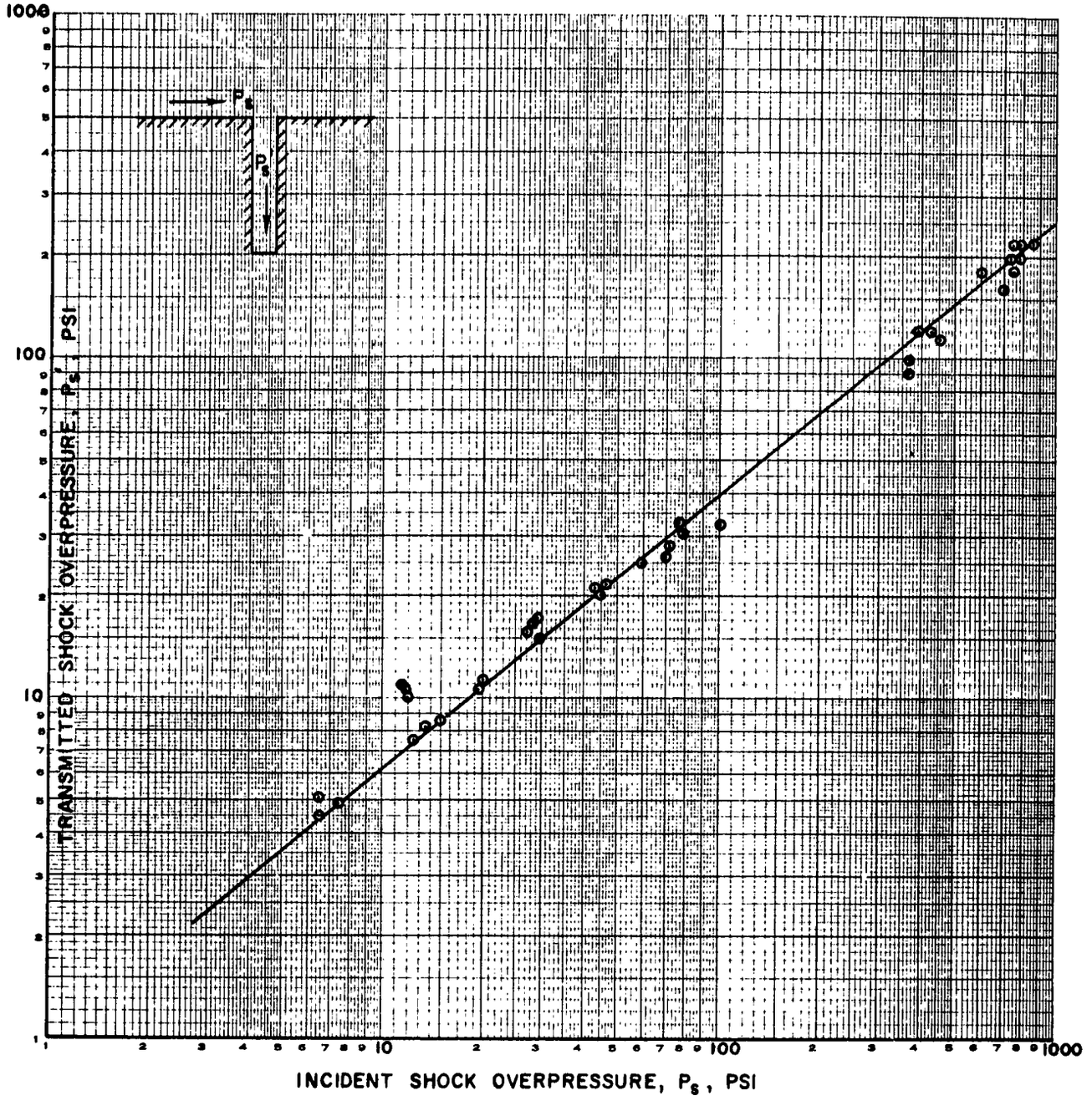

FIG. 3.4 - INCIDENT vs. TRANSMITTED SHOCK OVERPRESSURE FOR SIDE-ON TUNNEL

3.2.2 Exceptions for the Side-On Tunnel

When a tunnel is side-on to the incident shock wave but close enough to a large reflecting wall for the reflected pressure region to exist at the entrance to the tunnel, the entrance condition is, for all practical purposes, the same as the face-on case, and Figure 3.2 should be used for predicting the transmitted pressure. Figure 3.5 (a) and (b) shows a sketch of entrance configurations of this type, and the idealized pressure time curve. When the distance from the tunnel to the wall is equal to or less than the height of the wall as shown in sketch (a) one may assume the reflected condition. The effect will be a transient one because the reflected wave dissipates quickly.

In this case the transmitted wave will be initially complex, since it contains components of both the incident and the reflected waves (see Figure 3.5 (b). The interval between the two peaks shortens with time and will depend upon the incident pressure, the distance from the tunnel to the wall, and the distance the transmitted shock wave has moved down the tunnel. Finally they will coalesce to form one shock.

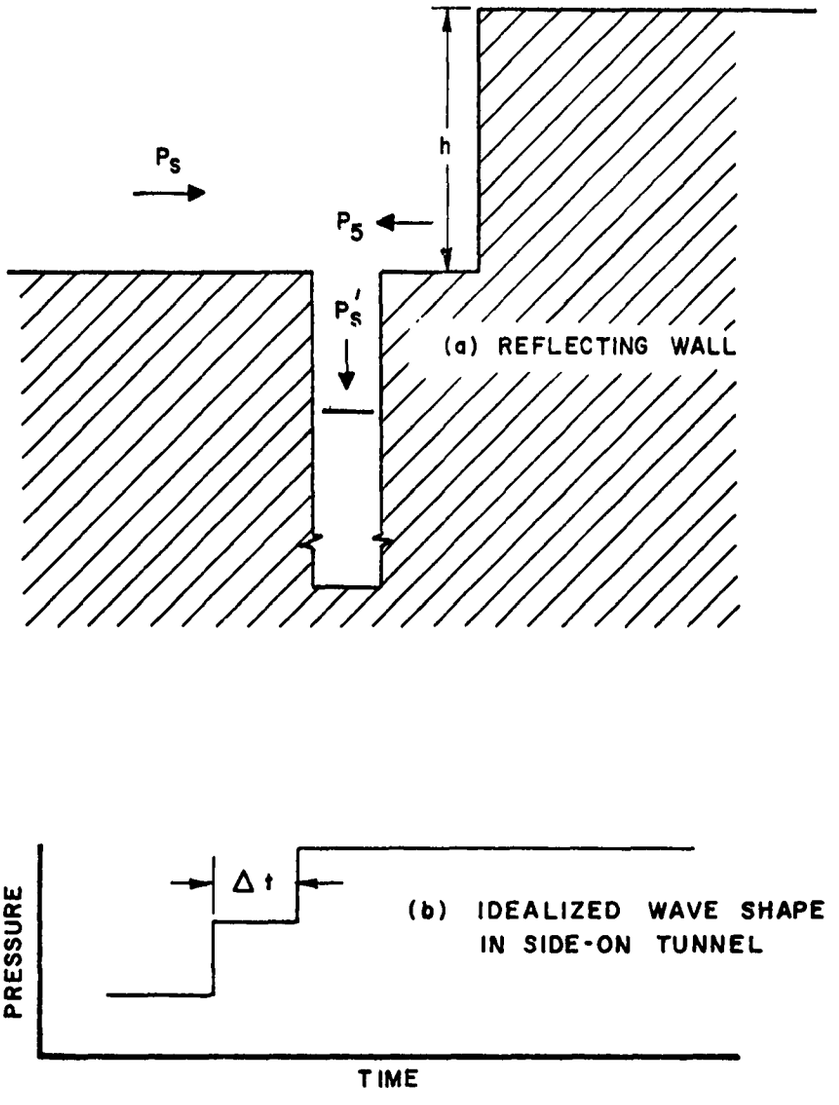

FIG. 3.5
SIDE-ON CONFIGURATIONS WITH REFLECTED PRESSURES

3.3 The Oblique Tunnel

When a shock wave impinges on a tunnel entrance, surrounded by an infinite baffle, at angles other than 0 and 90 degrees the pressure transmitted into the tunnel can be predicted from Figure 3.6. The values obtained at 0 and 90 degrees from Figure 3.6 will be the same as those obtained from the face-on and side-on conditions respectively (see Figures 3.2 and 3.4).

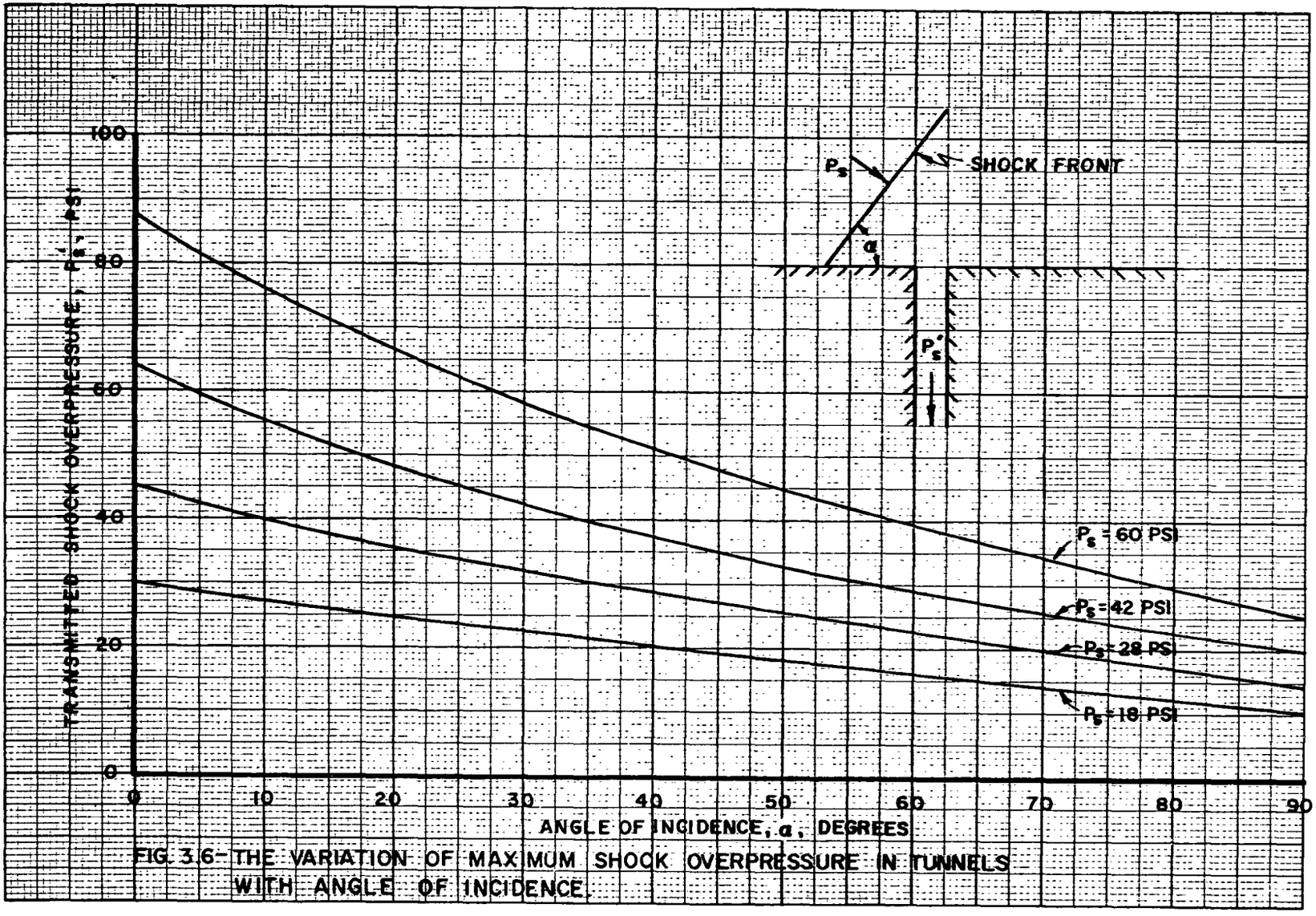

FIG. 3.6- THE VARIATION OF MAXIMUM SHOCK OVERPRESSURE IN TUNNELS WITH ANGLE OF INCIDENCE

4. TUNNEL JUNCTIONS

The intersection of one or more tunnels is termed as junction. Here the shock wave in the main tunnel generates shock waves in the secondary tunnels. This section presents experimental data which show the pressures which may be expected downstream of particular tunnel junctions. Throughout this section the term primary tunnel refers to the tunnel in which the shock conditions are known. The tunnels after a junction will be known as secondary tunnels.

4.1 Side-On Tunnel Junctions

4.1.1 The Tunnel Side-On to an Equal Area Tunnel

When a tunnel joins an equal area tunnel at 90°, the curve shown in Figure 4.1 should be used to predict the pressure in the secondary tunnel. Note that the pressures predicted from this curve are less than those shown in Figure 3.4 where there is essentially an infinite supply of air at the entrance of the tunnel.

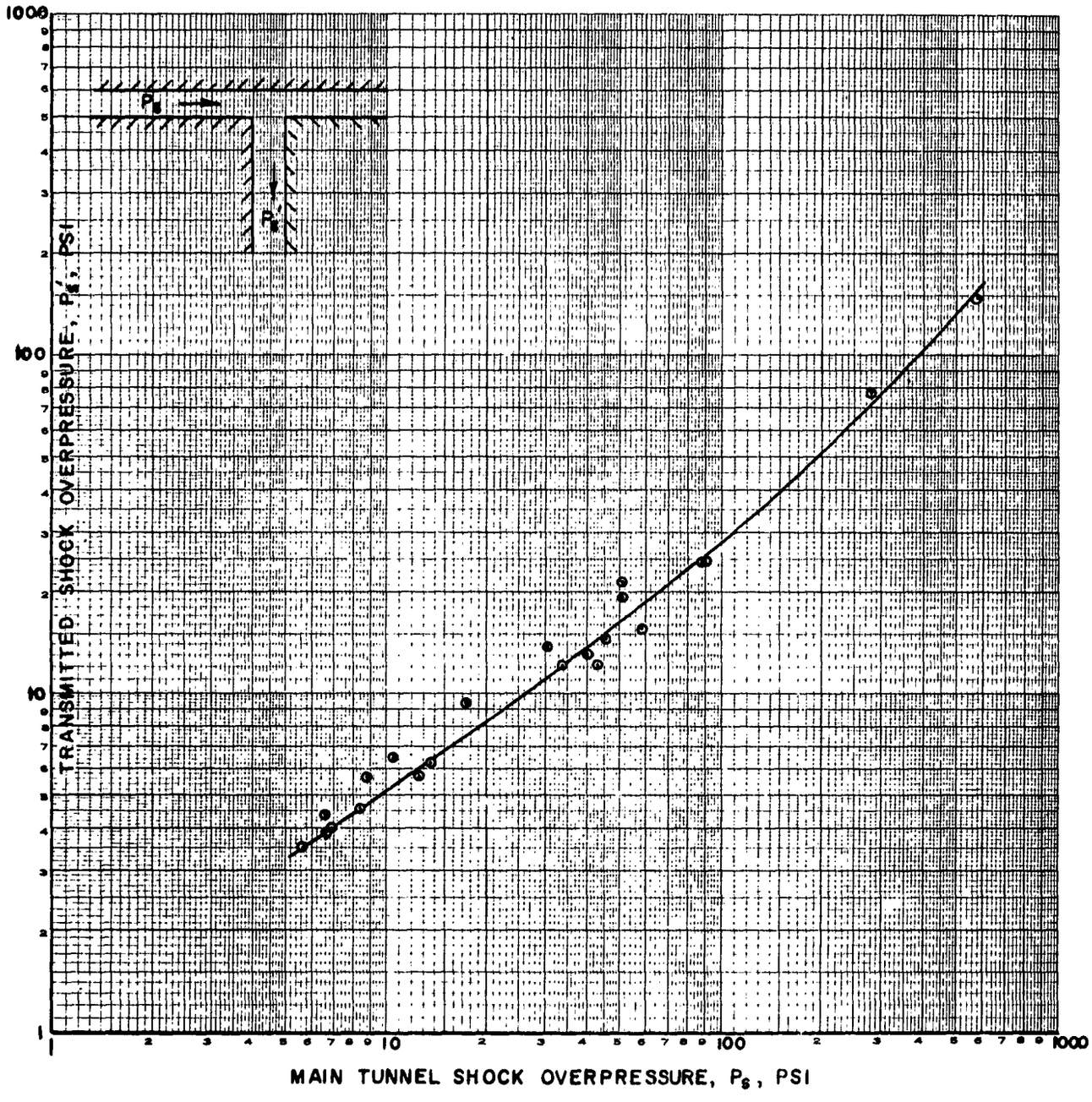

FIG. 4.1 – INCIDENT vs. TRANSMITTED SHOCK OVERPRESSURE FOR TUNNEL JOINED TO AN EQUAL AREA TUNNEL

4.1.2 The Tunnel Side-On to a Tunnel of Larger Area

As of this writing, no complete information can be presented in answer to this problem. This information is now being gathered and will be presented at the earliest possible time. It however is worthy of mention at this time that as an upper limit in the case of a small tunnel side-on to an extremely large tunnel, Figure 3.4 may be used to predict the pressure developed in the secondary tunnel.

4.2 The Pressure in the Primary Tunnel After a 90° Tunnel of Equal Area

Figure 4.2 can be used to predict the pressure in the primary tunnel after its intersection with a secondary tunnel which has an axis perpendicular to the axis of the primary tunnel.

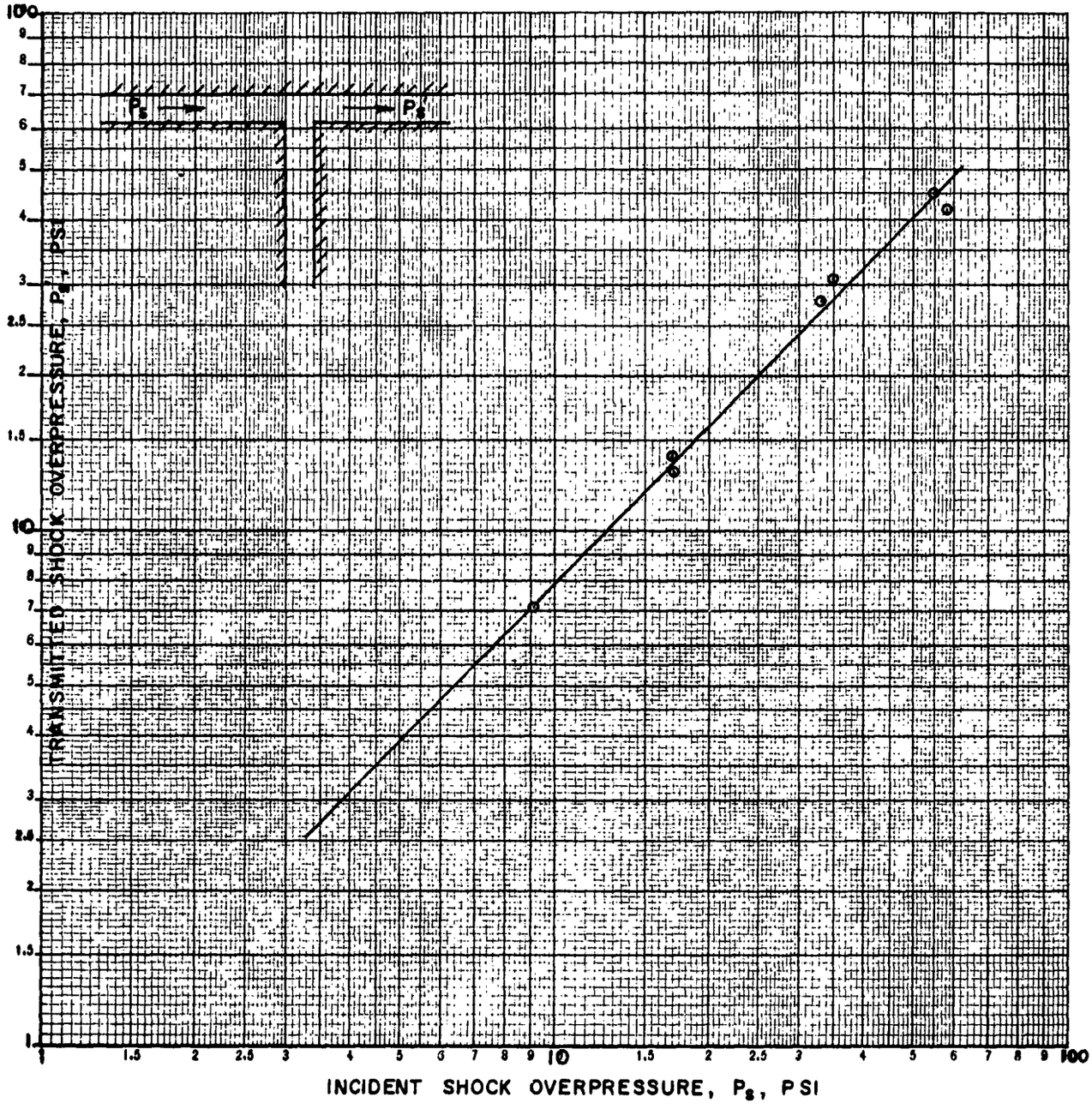

FIG. 4.2 – INCIDENT SHOCK OVERPRESSURE vs. SHOCK OVERPRESSURE TRANSMITTED DOWNSTREAM OF AN EQUAL AREA TUNNEL JUNCTION

4.3 The "T" Junction

Figure 4.3 shows a curve which may be used to predict the pressures that are obtained in the two secondary tunnels of a "T" configuration, when a shock wave is directed down the stem of the "T".

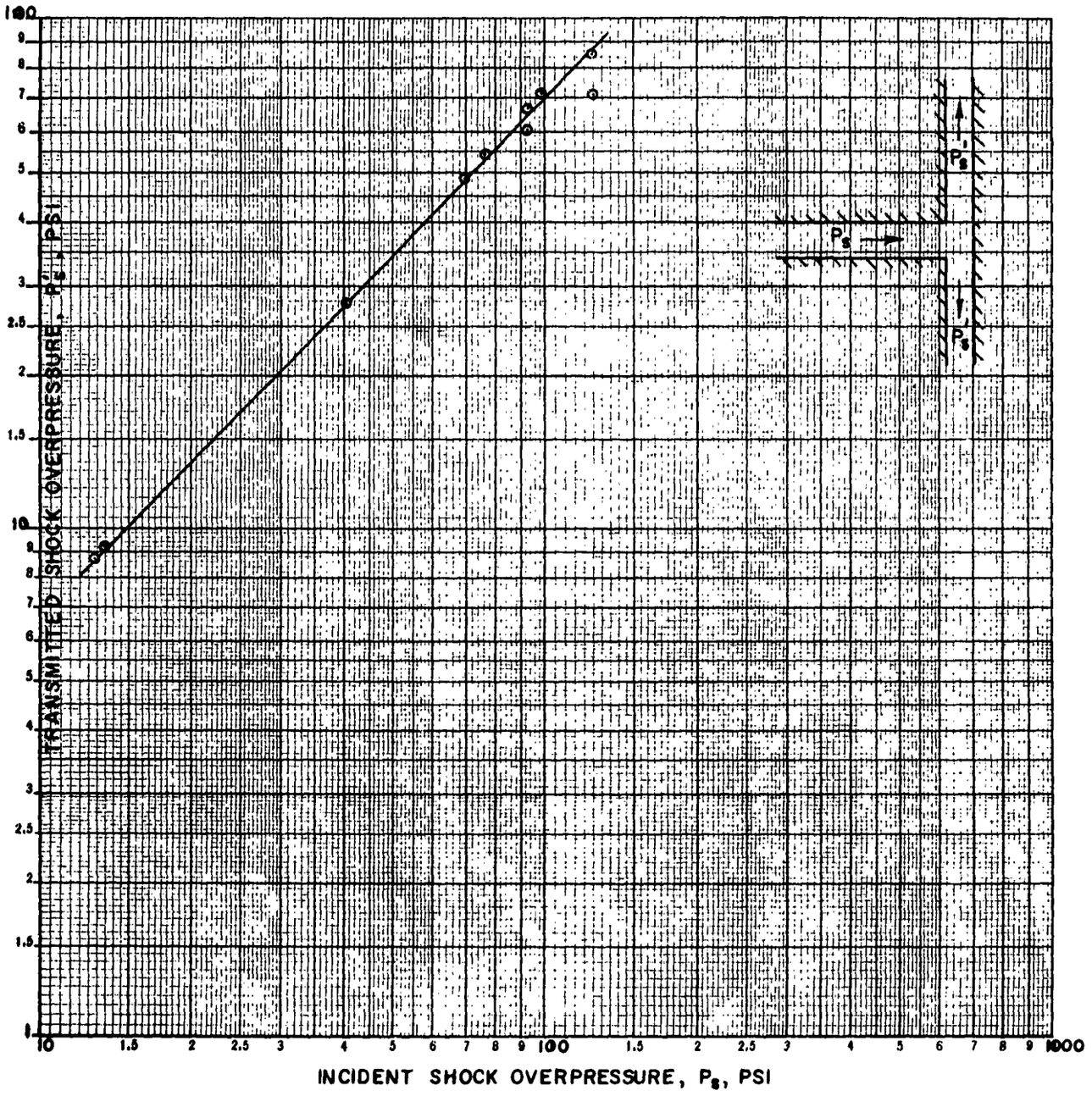

FIG. 4.3 - INCIDENT SHOCK OVERPRESSURE vs. TRANSMITTED SHOCK OVERPRESSURE FOR A "T" TUNNEL JUNCTION WITH EQUAL AREA TUNNELS

4.4 The "Y" Junction

Figure 4.4 may be used to predict the pressures in the two secondary tunnels of a symmetrical "Y" tunnel configuration.

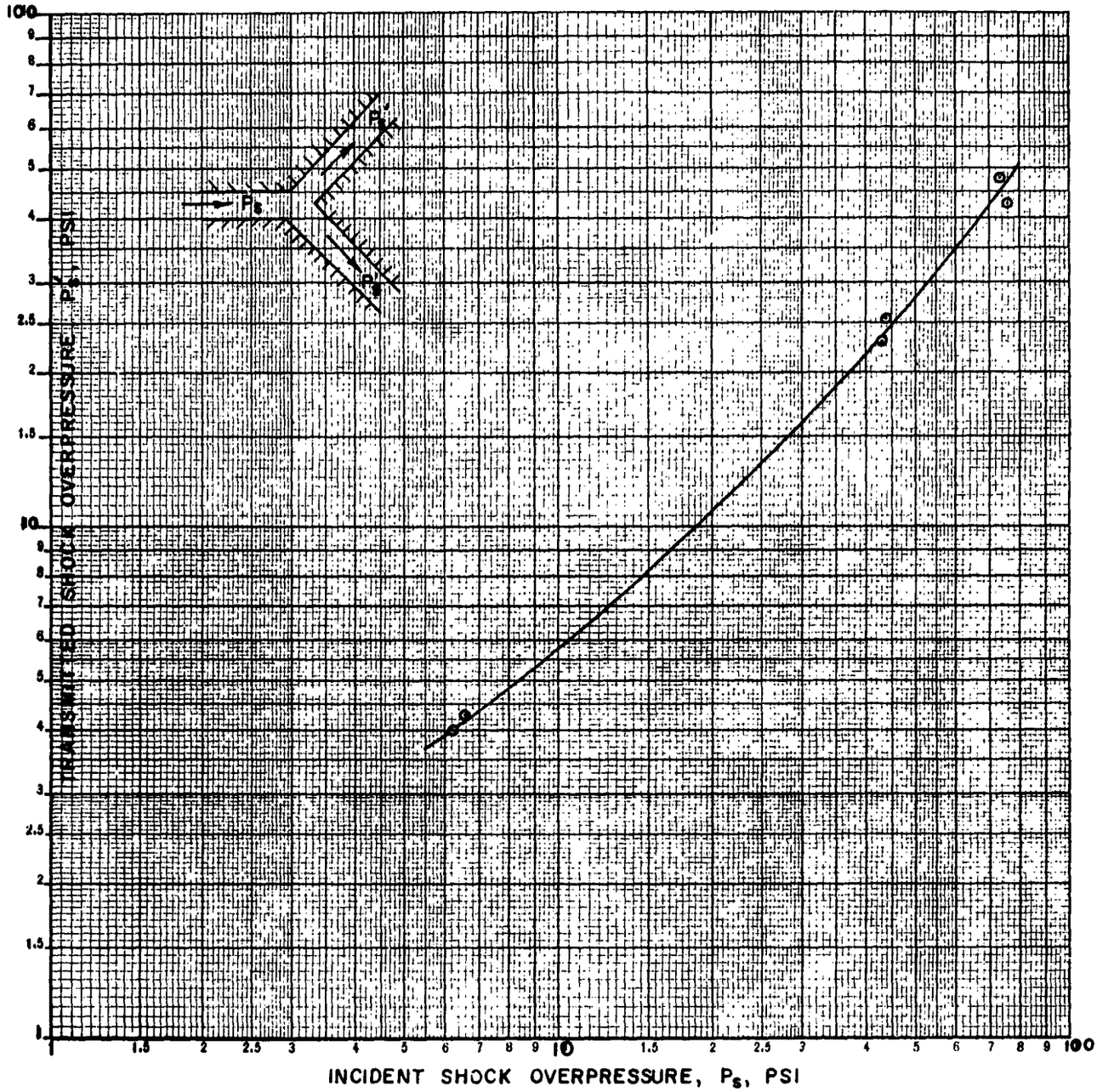

FIG. 4.4 - INCIDENT vs. TRANSMITTED SHOCK OVERPRESSURE FOR A "Y" TUNNEL CONFIGURATION

4.5 The "Cross" (+) Tunnel

Figure 4.5 shows the pressures which may be expected in the secondary tunnels of a cross. The figure shows two curves; one for the tunnels which have axes perpendicular to the primary tunnel and one for the secondary tunnel which is an extension of the primary tunnel, through the junction.

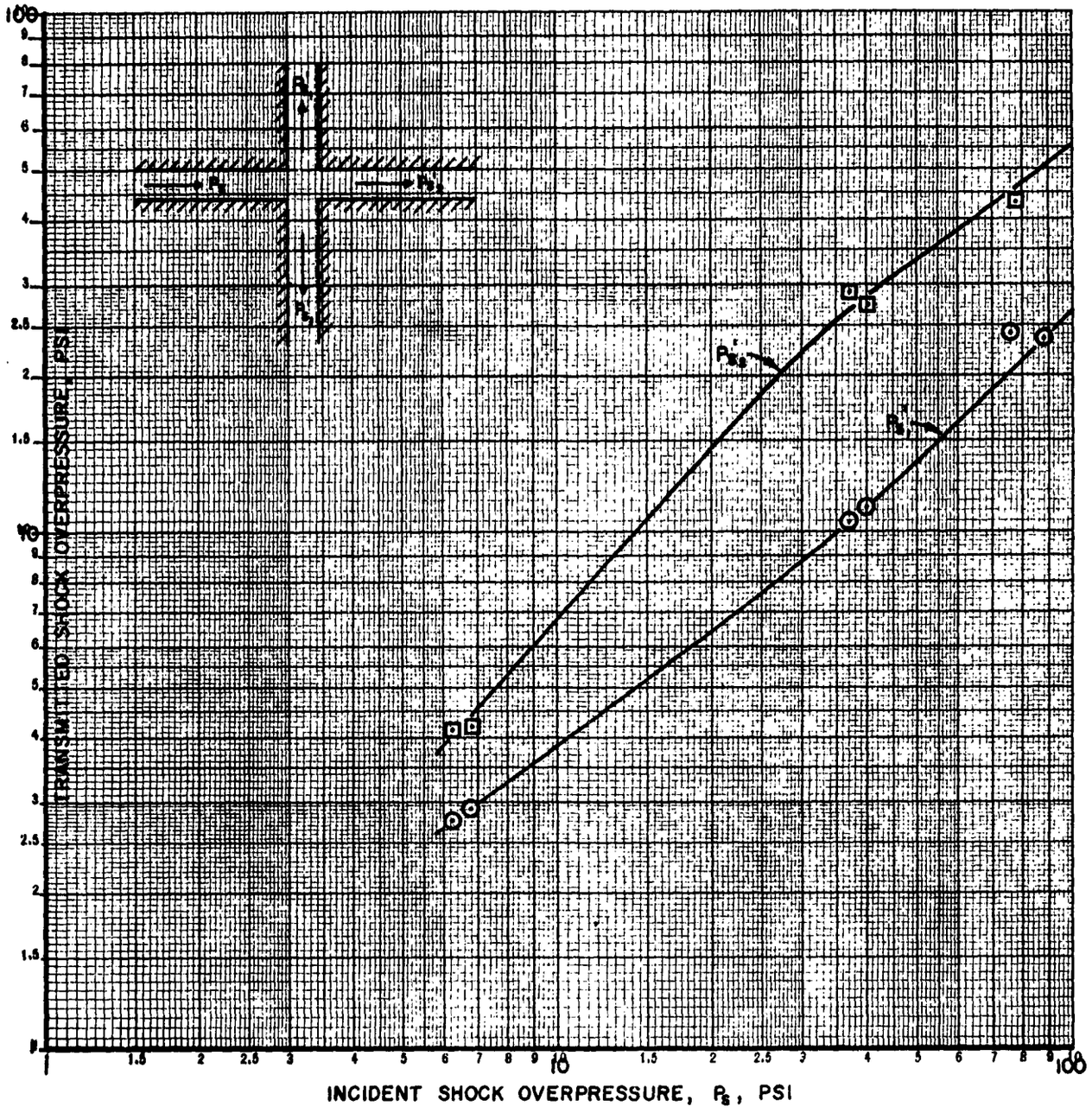

FIG. 4.5 – INCIDENT VS. TRANSMITTED SHOCK OVERPRESSURE FOR A CROSS, "+" TUNNEL CONFIGURATION

5. THE ATTENUATION OF A SHOCK WAVE IN A TUNNEL

When a peak shock wave travels through a tunnel the overpressure of the shock front will attenuate due to the one dimensional expansion of the shock wave and because of viscous interaction between the shock wave and the tunnel wall. The one dimensional expansion is governed by the wave shape, and the decay due to viscosity effects is a function of the roughness of the tunnel wall.

This chapter presents a theoretical equation which can be used in determining the attenuation in a tunnel, and the equation has been reduced to a nomograph so that problems can be readily worked. It should be applied only to smooth wall tunnels, however, because it is based on experiments with smooth wall pipes. When this equation is applied to rough wall tunnels it will predict an over estimate of the pressure.

5.1 Predicting the Attenuation of a Shock Wave in a Tunnel

In order to predict the attenuation of a blast wave, a time intercept (τ) must be determined. This would most effectively be accomplished by constructing a pressure-time curve of the blast wave in the tunnel and drawing a tangent to the profile immediately behind the shock front. The time interval between the front and the intersection of the tangent line with the base line (atmospheric pressure) is the time intercept, (Figure 5.1). In the event that this wave shape is not available, the τ for the shock wave before entrance into the tunnel may be used.

The pressure in the tunnel at the start should be given in Chapter 3. In addition, the perimeter of the tunnel, S (ft), the cross-sectional area of the tunnel, A (ft^2), the distance the shock wave is to travel in the tunnel, x (ft) and the value of the constant, K, which is a function of the overpressure of the shock wave determined from Figure 5.2, must be known.

Substituting these known parameters into the equation

$$P_{s_x} = P_s' \exp - \left[\frac{7S}{A} + \frac{1}{\tau + \frac{x}{4a_1}\left(1 - \sqrt{\frac{7P_1}{7P_1 + 6P_s'}}\right)} \right] Kx \qquad \text{Eq 5.1}$$

and solving the equation for P_{s_x} gives the pressure remaining after a travel of x distance down the tunnel.

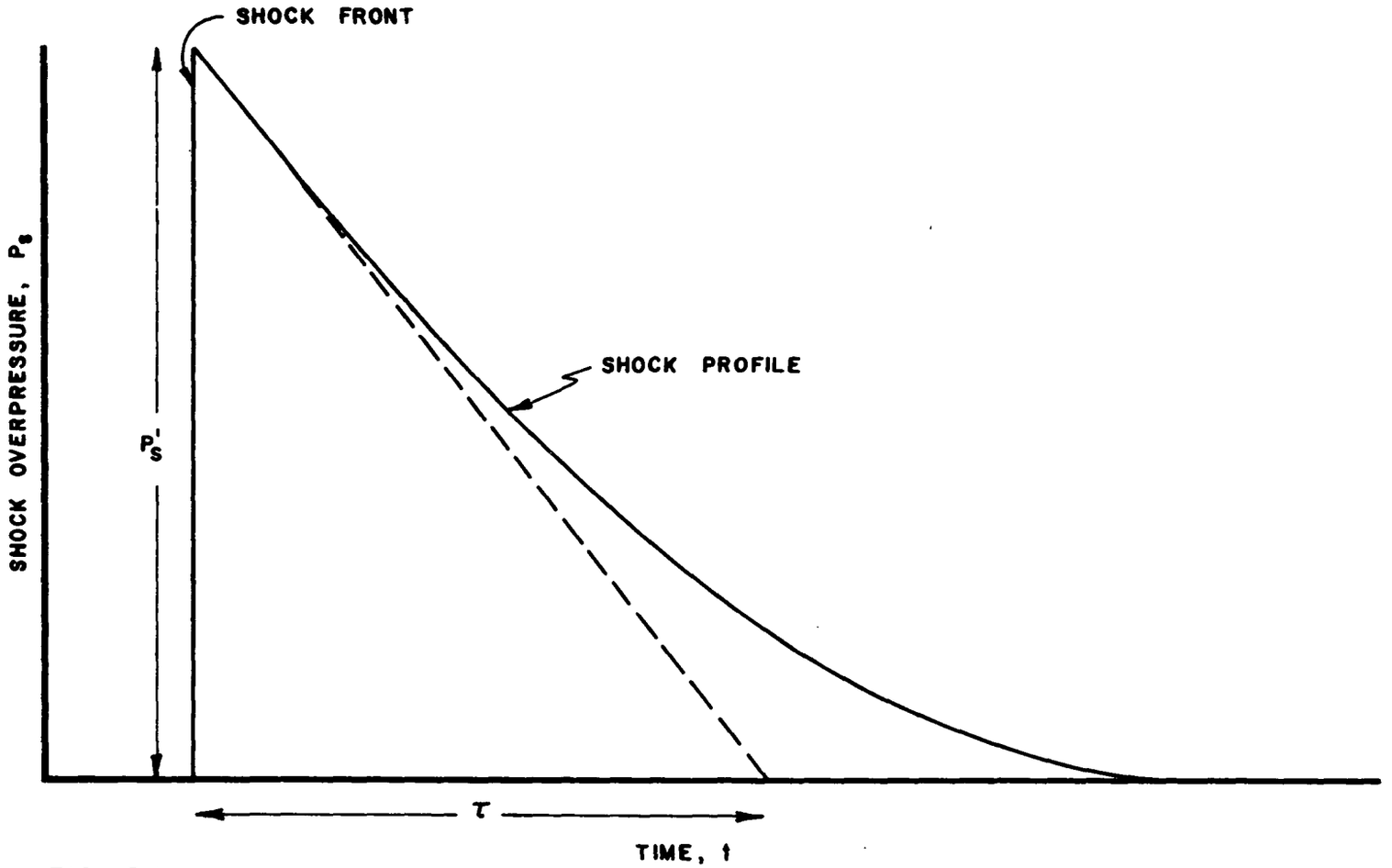

FIG. 5.1
A TYPICAL PRESSURE-TIME RECORD OF A SHOCK WAVE WITH TANGENT DRAWN TO INDICATE THE TIME INTERCEPT.

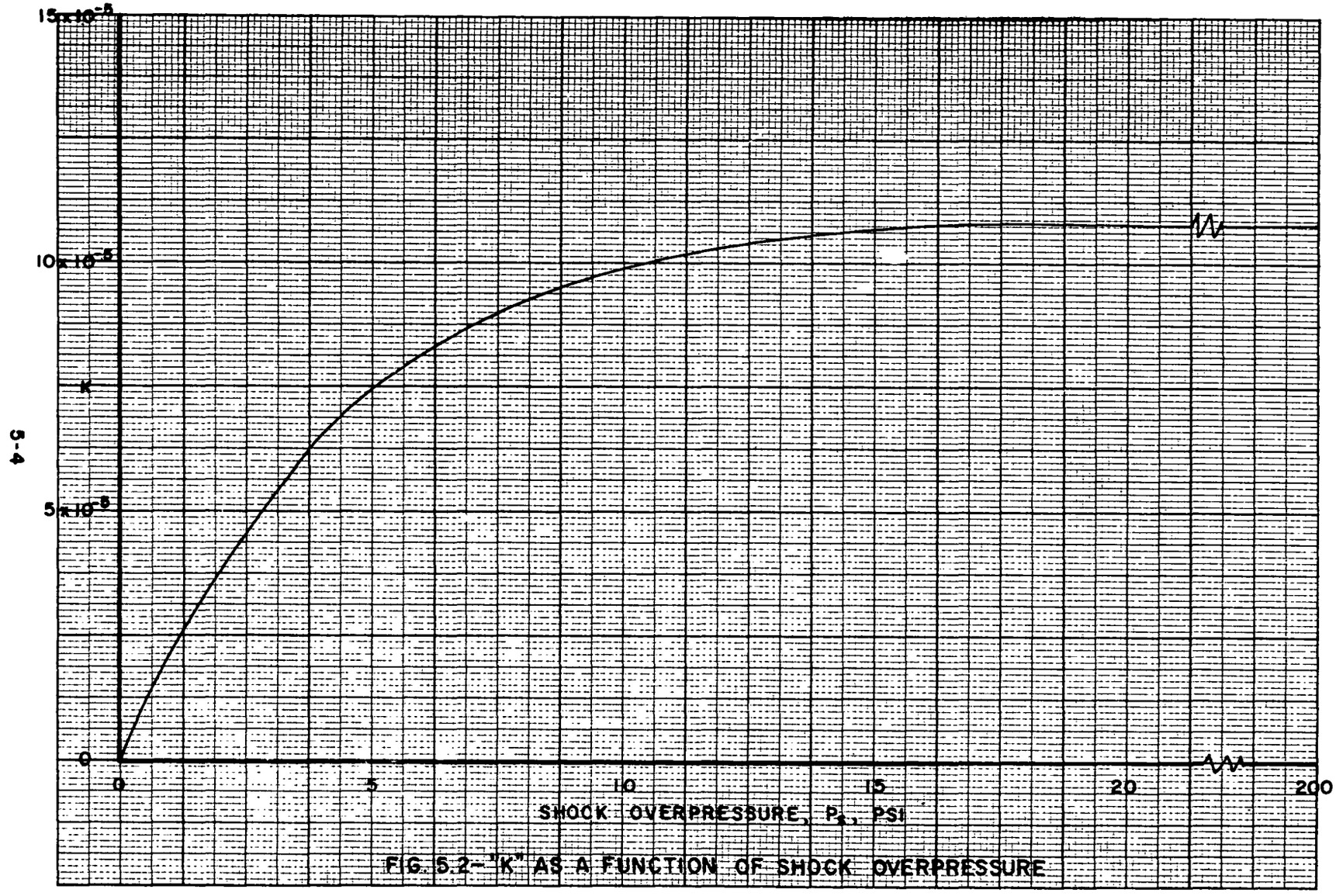

FIG. 5.2 - "K" AS A FUNCTION OF SHOCK OVERPRESSURE

5.2 Predicting the Duration of a Shock Wave in a Tunnel

When a shock wave passes down a tunnel, viscous effects act on the wave in such a way as to decrease the slope of the wave immediately behind the front. This is a result of the dissipation of kinetic energy toward the rear of the wave, and hence it cannot contribute to the support of the shock front. Therefore, the actual pressure-time profile, measured at a point other than the entrance, shows a larger time intercept than what should be used to calculate attenuation due to expansion alone.

After an attenuation due to travel of the shock wave down the tunnel, there will be two time intercepts associated with the shock wave. One of these time intercepts will be that presented to the remainder of the straight uniform tunnel, and the second will be that presented side-on to any sort of tunnel junction.

The time intercept presented to the remainder of the straight uniform tunnel, τ' , will be that obtained from the equation

$$\tau' = \tau + \frac{x}{2a_1}\left(1 - \sqrt{\frac{7P_1}{7P_1 + 6P_s}}\right) \qquad \text{Eq. 5.2}$$

The time intercept presented side-on to any type of tunnel junction, τ'', will be given by

$$\frac{1}{\tau''} = \frac{1}{\tau'} - \frac{(5/2)(P_{s_x})}{\Phi D(7P_1 + P_{s_x})}, \qquad \text{Eq. 5.3}$$

where Φ = 0.13 sec/ft., and P_{s_x} is the pressure at x from equation 5.1.

5.3 Determining the Attenuation in a Tunnel From a Nomogram

Figure 5.3 is a nomogram that can be used for the determination of the pressure remaining after the shock wave has traveled down a tunnel for a given distance. Directions for the use of this nomogram are given in Figure 5.3. When using the nomogram for the determination of attenuation, the limit of the input parameters should be kept in mind. The limits are: P_s' from 10 psi to 1000 psi, x from 10 feet to 1000 feet, τ from .5 sec. to 5 sec. and the diameter of the tunnel from .5 feet to 30 feet.

When the tunnel to be considered has a round cross-section the nomogram can be used directly, but if the tunnel has a cross section other than circular, the use should be modified as follows. Rather than using Step 5 of the directions involving scales F and G, the value of $\frac{7S}{A}$ for the tunnel should be used as the value of scale G and the directions followed as usual from Step 6 on.

Since the distance scale on the nomograph is a maximum at 1000 feet it will be necessary to treat very long tunnels in 1000 foot intervals and when this is the case use Equation 5.2 for computing a new time intercept for the new increment. A simple calculation has been made on the nomogram using the input parameters indicated on the work sheet and the values of this sample are also indicated on the work sheet.

1. Determine the values of the input shock overpressure, the time intercept of the input shock wave, the diameter of the tunnel and the distance the shock wave is to travel in the tunnel. Record these values with the proper units in the appropriate places on the work sheet.

2. Locate the values of the input shock overpressure and the travel distance on scales A and B respectively. By placing a straight edge along the values on scales A and B, read the indicated value on scale C. Record this value on the work sheet.

3. To the value read from scale C add the value of the time intercept and record the sum on the work sheet in the space indicated as scale D.

4. Locate the value of scale D on its respective scale and read the corresponding value from scale E. Record this value on the work sheet.

5. Locate the value of the tunnel diameter on scale F and read the corresponding value on scale G. Record this value from scale G on the work sheet.

6. Add the values from scales E and G and record the sum on the work sheet in the space indicated as scale H.

7. Multiply the travel distance by 0.00011 and enter this on the work sheet in the space indicated as scale I.

8. Locate the values of scales H and I on their respective scales. By placing a straight edge along the values on scales H and I read the indicated value on scale J. Record this value on the work sheet.

9. Divide the value of the input shock overpressure by the value on scale J and record this value on the work sheet as P_{s_x}, the pressure remaining after a travel of x distance down the tunnel.

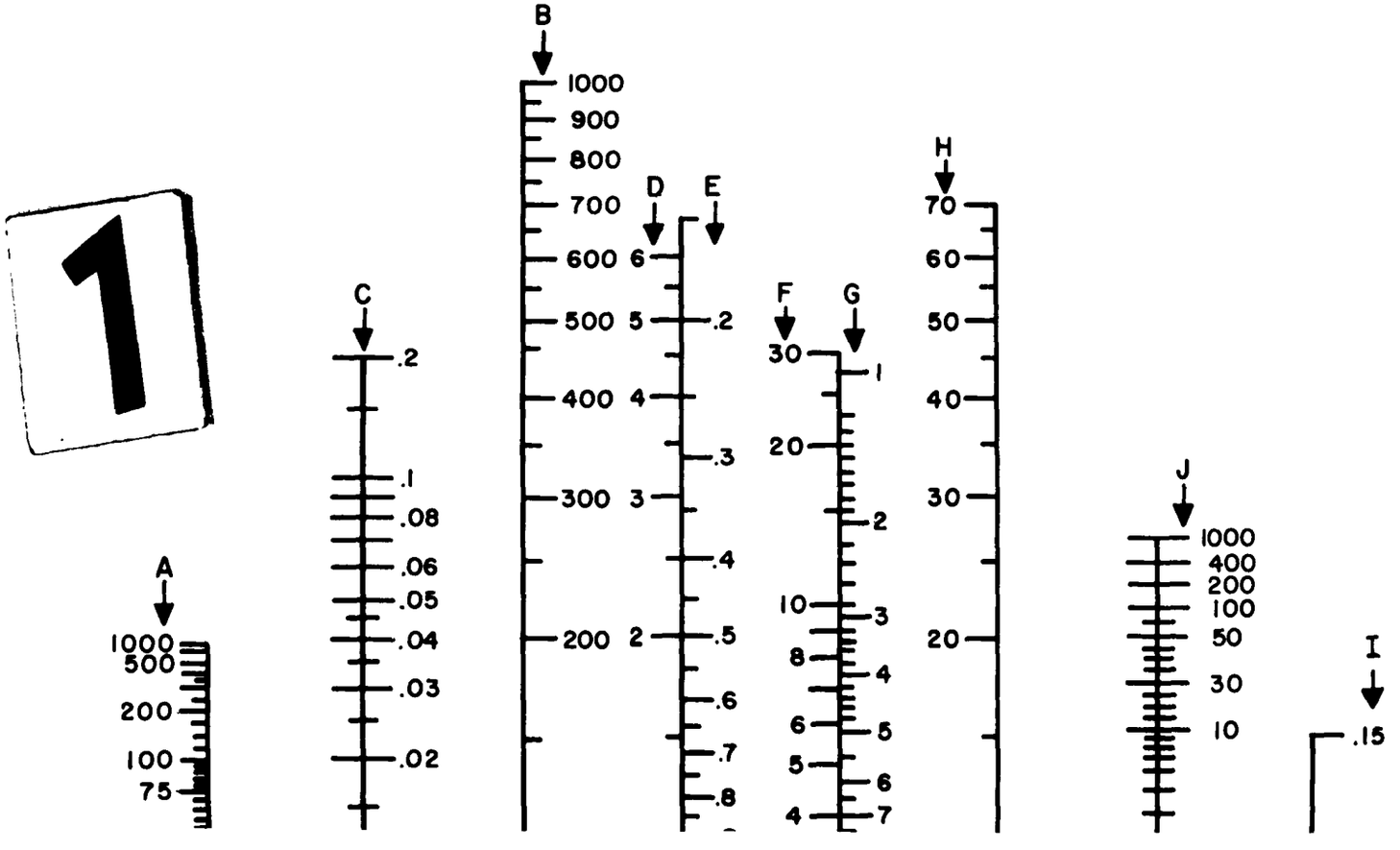

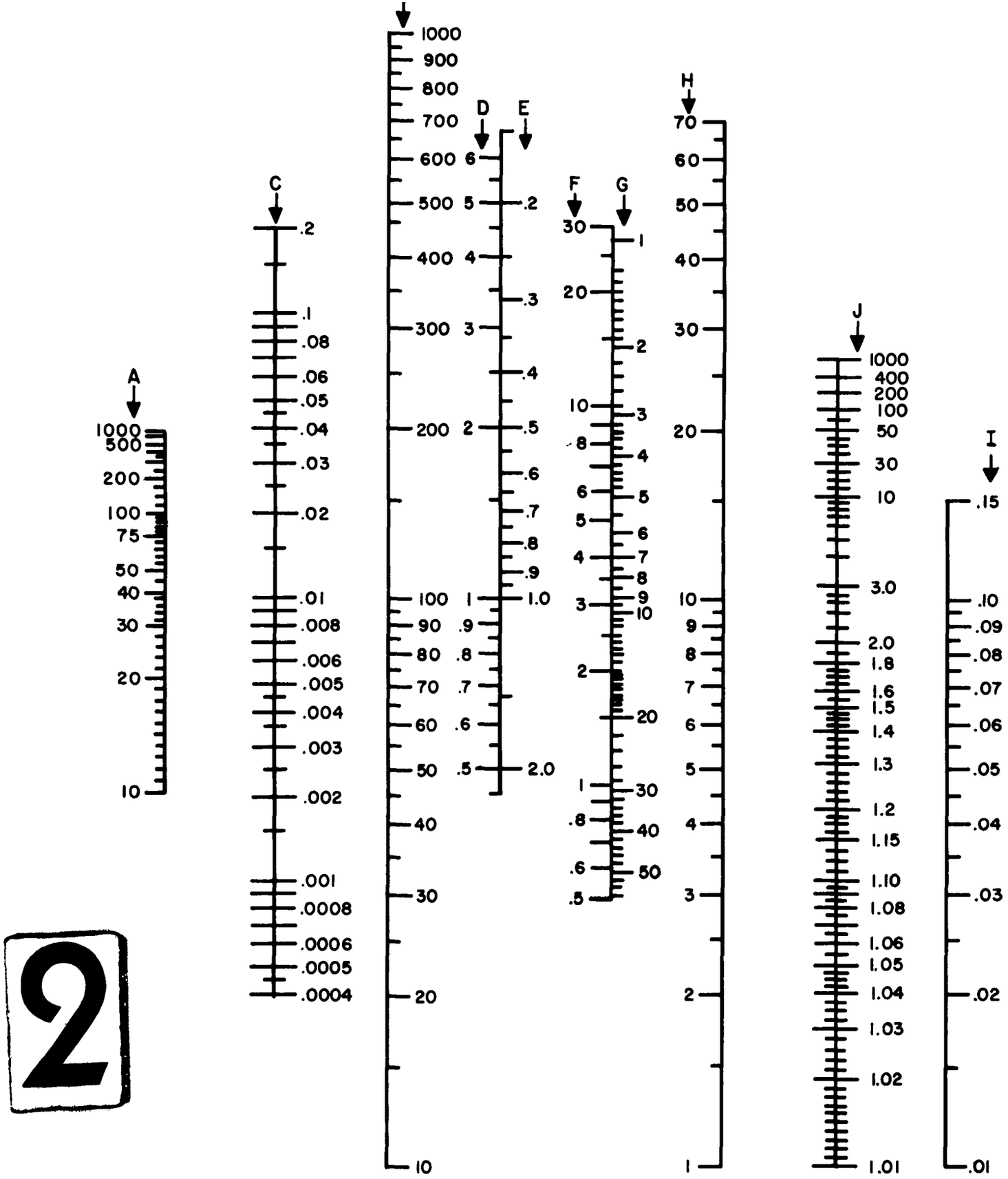

FIG. 5.3– NOMOGRAM FOR DETERMINING THE ATTENUATION OF A SHOCK WAVE TRAVELING IN A TUNNEL.

WORK SHEET

Input Shock Overpressure, psi.	100				
Travel Distance, ft.	1000				
Time Intercept, sec.	1				
Tunnel Diameter, ft.	10				
Scale C	0.14				
Scale D	1.14				
Scale E	0.95				
Scale G	2.80				
Scale H	3.75				
Scale I	0.11				
Scale J	1.48				
P_{s_x}, psi.	67.8				

6. AREA CHANGES IN TUNNELS

As might be expected, when a shock wave travels through a section of transition in a tunnel, it will experience some change due to the transition. This change, either an increase or decrease in the shock pressure will depend upon the nature of the transition and also upon the extent of the transition. At present the experimental data on area changes is very limited however experiments are in process so new information is forthcoming.

6.1 Area Increases in Tunnels

A shock wave passing through an area increase in a tunnel undergoes a decrease in pressure. For a long duration or step incident wave, the transmitted wave is always peaked close to the area change, but after several diameters of the new increased area, the wave tends to flatten out. In all cases, the strength of the wave decreases after passing into a larger area tunnel.

If the flow behind the incident wave is initially supersonic, that is, greater than about 56 psi, a shock is transmitted and an upstream facing shock forms in the transition section. This shock either stands in some part of the transition section or is swept downstream into the larger area tunnel, depending on the area ratio and the strength of the incident wave. The upstream facing shock formed by the expansion affects the pressure history close to the transition section. The transmitted pressures shown in Figure 6.1 are several diameters downstream of the transition, where the peak has disappeared and the wave is again flat.

Shock tube experiments to date show that the ratio of input pressure to transmitted pressure is dependent only on the input pressure ratio and the area ratio. The diameter of the small and large ducts do not affect the results provided that the area ratio is kept constant.

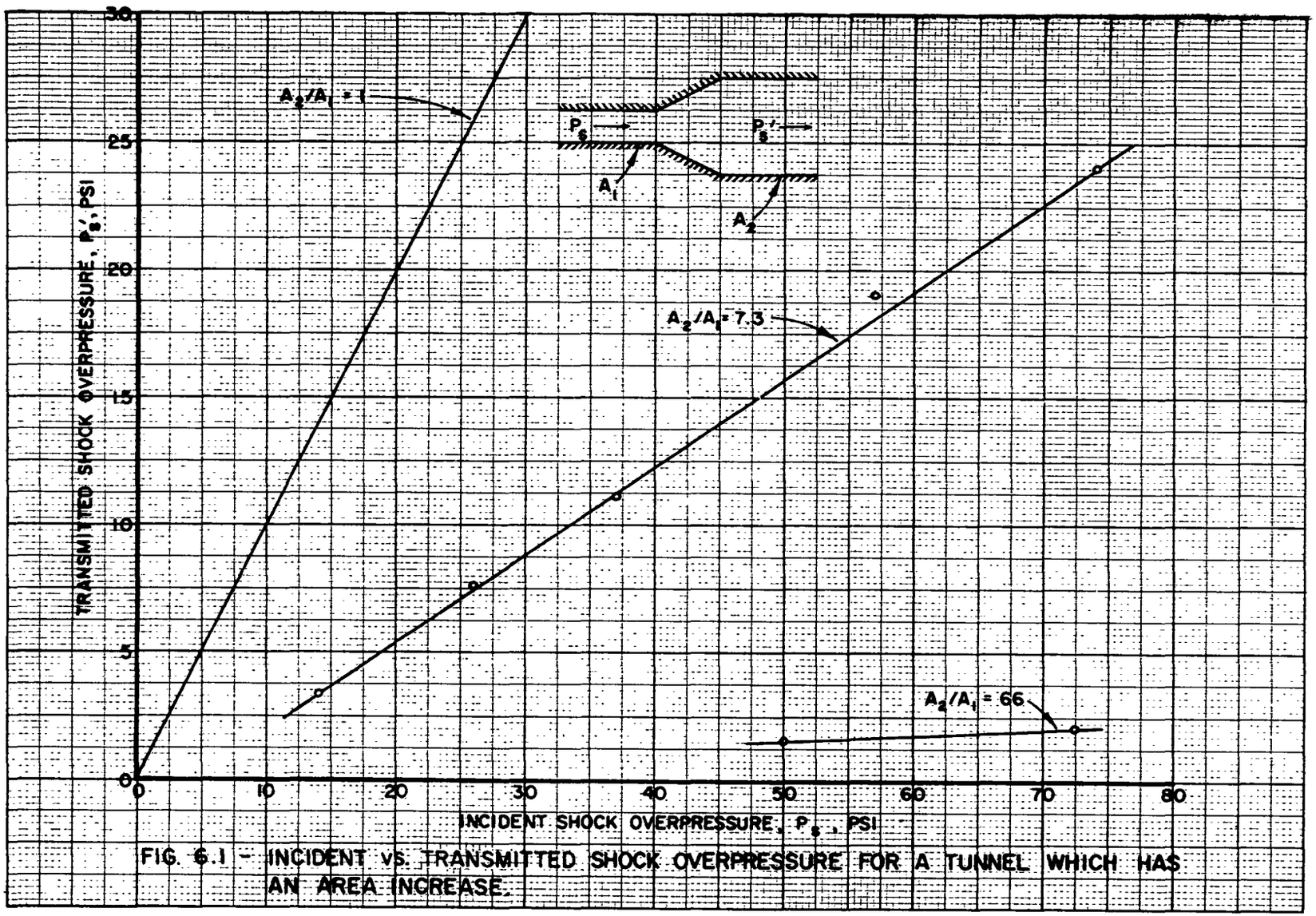

FIG. 6.1 – INCIDENT vs. TRANSMITTED SHOCK OVERPRESSURE FOR A TUNNEL WHICH HAS AN AREA INCREASE.

7. SHOCK WAVE FILLING A CHAMBER THROUGH TUNNEL SYSTEMS

When a shock wave is applied to a tunnel system, the resulting wave action within the system will depend on the geometry of the system. In general, a shock wave will initiate a transient or non-steady process which consists of the primary shock front followed by compression waves, rarefaction waves and shock fronts reflecting from open and closed tunnel ends. During the passage of these transient waves, the pressure throughout the system gradually increases as a result of flow into chamber volumes. This flow is called quasi-steady because it tends to conform to steady flow theory.

A good example of the non-steady process is seen in the idealized pressure-time curve, Figure 7.1, taken from a gage located part way down a straight tunnel, closed at one end and exposed to a step shock at the other end. The curve shows a series of six distinguishable pressure levels; the last four indicated as 3, 4, 5, and 6 on Figure 7.1 will recycle with decaying amplitude. If a chamber is added to this tunnel system, the relatively high frequencies represented in the transient waves will be attenuated due to absorption by the chamber. The absorbing quality of a chamber will depend on how much of the initial shock is taken from the tunnel system and not returned by the chamber. For example, a small chamber at the end of a tunnel will take all of the initial shock, but will return, in the way of reflection, some of it to the tunnel system. However, a large chamber will take all of the initial shock and reflect but a small portion. A chamber located part way up a tunnel and connected to the side wall of the tunnel with a short duct will take only part of the initial shock front and allow the rest to

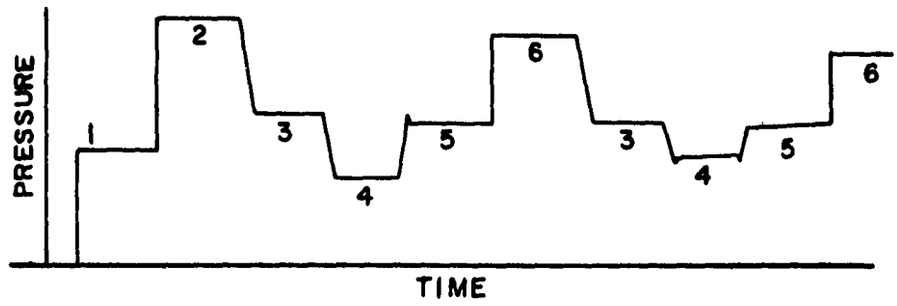

1. The primary shock passes into the tunnel increasing the pressure.

2. A reflection of the primary shock from the closed end moves back up the tunnel to the open end, again increasing the pressure.

3. The reflected pressure is relieved at the open end by a rarefaction wave which moves back into the tunnel and reduces the pressure.

4. Reflection of this rarefaction at the closed end, result in a stronger rarefaction again lowering the pressure.

5. When this low pressure reaches the open end, a compressional wave is allowed to enter the tunnel and move toward the closed end and increase the pressure again. This compressional wave may develop a shock front as it moves down the tunnel.

6. A reflection of this compressional wave at the closed end results in a stronger compressional wave moving toward the open end.

FIG. 7.1 - CYCLIC NATURE OF A SHOCK WAVE IN A CLOSED END TUNNEL.

continue in the main tunnel. In this case, the ratio of the volume of the chamber to the cross-sectional area of the tunnel will determine whether or not some of the wave entering the chamber is returned to the tunnel.

7.1 The Pressure-Time History in a Chamber

7.1.1 The Chamber Geometry

When a shock wave is applied to the entrance of a chamber which has roughly cubical dimensions, and the entrance area to the chamber is small compared to the volume of the chamber immediately behind the entrance, the chamber will fill to a maximum pressure in a time that is a function of the chamber geometry, volume, entrance area, and applied pressure. The shape of this pressure time curve will be treated in the next section.

7.1.2 Construction of the Fill-Time Curve

Figure 7.2 shows a curve of an experimentally determined quantity C versus $(P_s - P_4)$. This curve may be used to predict the pressure-time history in a chamber but only for those applied pressure waves whose overpressure is less than 150 psi.

Figure 7.3 shows a layout of a possible tunnel chamber configuration to which the method described can be applied.

The following steps should be taken in order to make a prediction of the pressure-time history within a chamber.

1. A typical pressure-time record of the applied wave must be obtained. This may be observed either from actual records of previous firings or by assuming the pressure and wave shape. This applied wave should be plotted on a pressure-time coordinate axis as done in Figure 7.4.

2. Specific values of overpressure should be read from this curve corresponding to selected values of time. In order for the person unaccustomed to working with this method to be successful, it is suggested that some twenty to forty time values be selected along the time axis. Also, for ease of calculation, it is suggested that these times be so selected as to give equal time intervals.

3. Take the value of P_s read for $t = 0$. From this value of P_s subtract the value of P_4 also for $t = 0$. It might be noted at this point that for $t = 0$, $P_4 = 0$, however for any value of $t > 0$, P_4 will be greater than 0.

4. Using this value of $(P_s - P_4)$ determine from Figure 7.2 the value of C for $t = 0$.

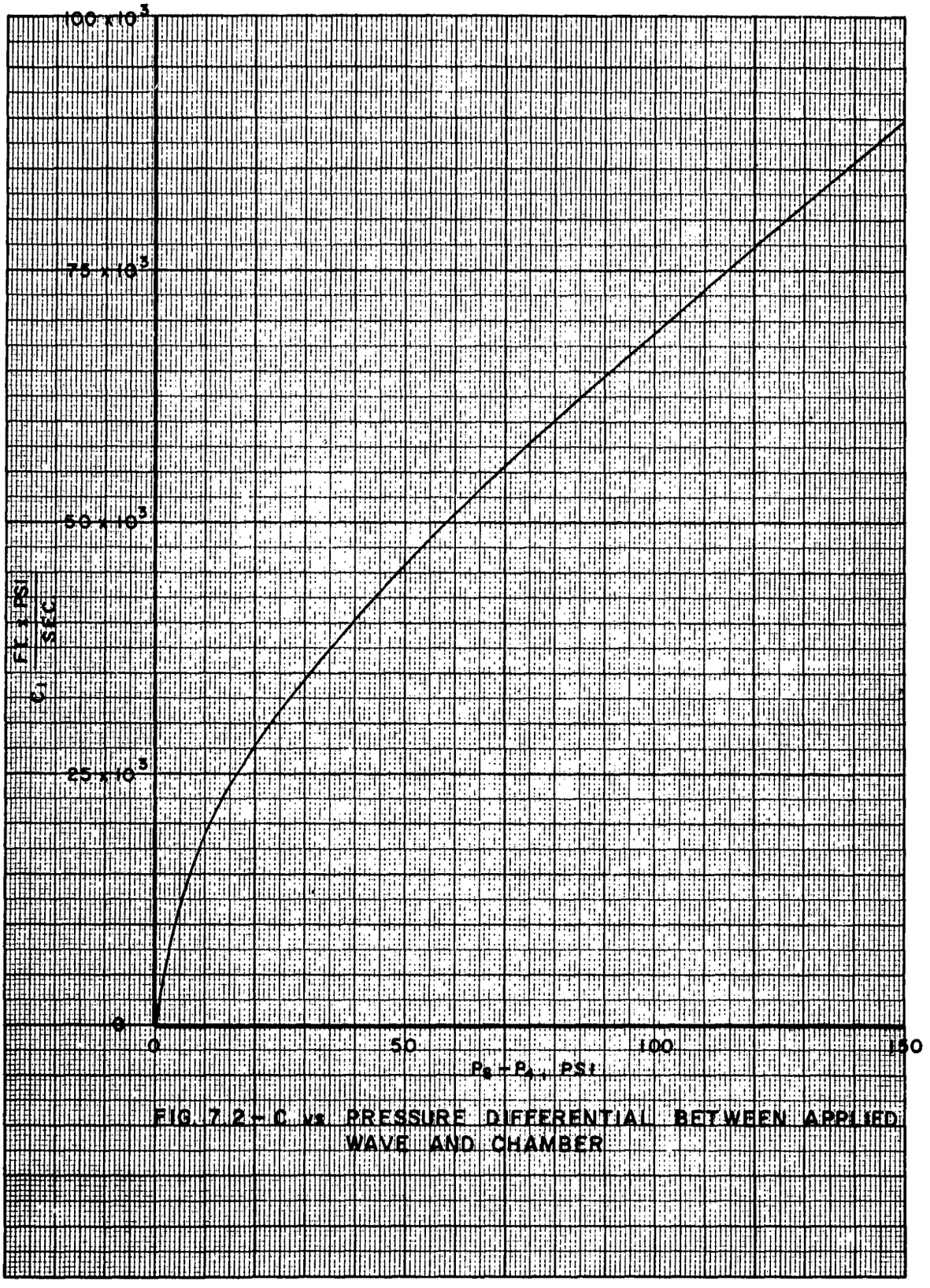

FIG. 7.2 - C vs PRESSURE DIFFERENTIAL BETWEEN APPLIED WAVE AND CHAMBER

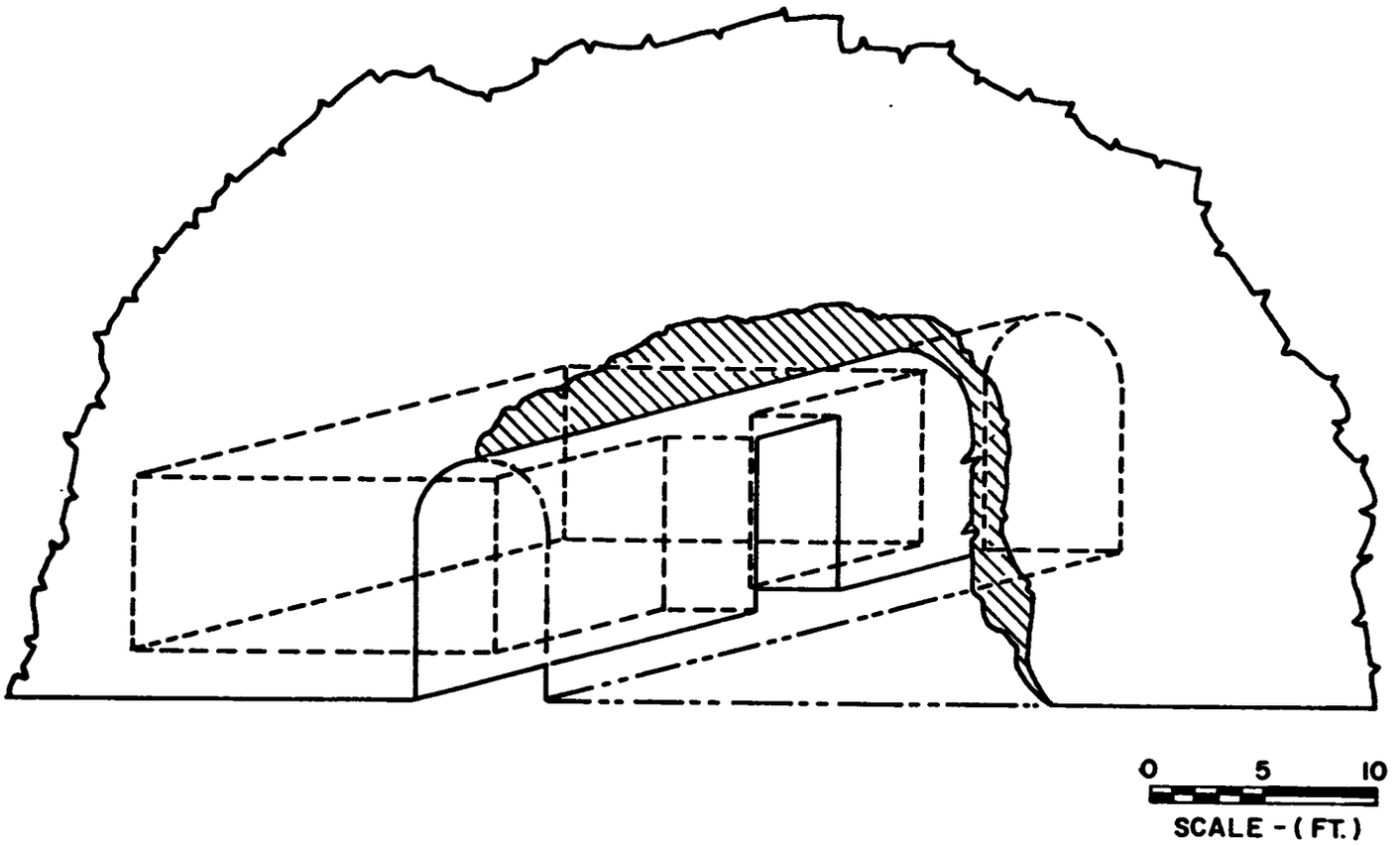

FIG. 7.3
TYPICAL TUNNEL ENTRANCE AND CHAMBER CONFIGURATION

5. Substitute the values of C, V, and A into the equation $C = \frac{V}{X} \times \frac{\Delta P_4}{\Delta t}$, where V is the volume of the chamber to be filled, A the area of the entrance to the chamber through which the filling takes place and Δt is the time in seconds between the value of $t = 0$ and the next value of t chosen in step 2. Solve the equation for ΔP_4.

6. Add ΔP_4 to the overpressure in the chamber at the beginning of the time interval. Note that the overpressure in the chamber at time $t = 0$ is zero. This summation of $P_4 + \Delta P_4$ will be the value of P_4 used in the second time interval.

7. On a convenient pressure-time axis, plot the obtained values of P_4 against the values of t in seconds at the end of the time interval. Draw a straight line connecting the preceding point and the one thus plotted. In the case of the first time interval, the straight line will be constructed between the origin and the first calculated point.

8. Determine the value of $(P_s - P_4)$ for the second time interval. This is done by reading the value of P_s corresponding to the second value of time selected and subtracting from this the value of P_4 in step 6.

9. Again as in step 4, find the corresponding C and solve the equation as in step 5.

10. Plot the second point and again connect this point and the preceding one with a straight line.

This process should be repeated for all time intervals selected in step 2. The resultant series of straight lines will give the pressure-time history in the chamber.

Table 7.1 and Figure 7.5 give a tabulation of the pressure time history and a plot of this history respectively. This tabulation and curve result when the shock wave in Figure 7.4 enters a chamber of the type shown in Figure 7.3 where the ratio of the volume of the chamber to the area of the entrance is 100. It should be pointed out here that when, in the course of the calculations, the value of $(P_s - P_4)$ becomes negative, Figure 7.3, the curve of $(P_s - P_4)$ versus C may still be used. However, when $(P_s - P_4)$ is negative it should be assumed that both axes of the curve are negative. Therefore a negative $(P_s - P_4)$ will give rise to a negative C.

Table 7.1 **Tabulation of a Pressure-Time History of a Chamber**

t, sec.	P_s, psi	P_4, psi	$P_s - P_4$	C	ΔP_4
0	20.0	0	20.00	28.0×10^5	7.00
.025	19.2	7.00	12.20	22.3	5.58
.050	18.4	12.58	5.82	15.0	3.75
.075	17.6	16.33	1.27	5.0	1.25
.100	16.8	17.58	-.78	-3.0	-.75
.125	16.0	16.83	-.83	-3.0	-.75
.150	15.2	16.08	-.88	-3.5	-.88
.175	14.5	15.20	-.70	-2.5	-.62
.200	13.8	14.58	-.78	-3.0	-.75
.225	13.1	13.83	-.73	-2.5	-.62
.250	12.4	13.21	-.81	-3.0	-.75
.275	11.8	12.46	-.66	-2.5	-.62
.300	11.2	11.84	-.64	-2.0	-.50
.325	10.6	11.34	-.74	-2.5	-.62
.350	9.9	10.72	-.82	-3.0	-.75
.375	9.4	9.97	-.57	-2.0	-.50
.400	8.8	9.47	-.67	-2.5	-.62
.425	8.3	8.85	-.55	-2.0	-.50
.450	7.7	8.35	-.65	-2.5	-.62
.475	7.2	7.73	-.53	-2.0	-.50
.500	6.7	7.23	-.53	-2.0	-.50
.525	6.2	6.73	-.53	-2.0	-.50
.550	5.7	6.23	-.53	-2.0	-.50

Table 7.1 (Continued)

t, sec.	P_s, psi	P_4, psi	$P_s - P_4$	C	ΔP_4
.575	5.2	5.73	-.53	-2.0×10^5	-.50
.600	4.8	5.23	-.43	-1.0	-.25
.625	4.4	4.98	-.58	-2.0	-.50
.650	3.9	4.48	-.58	-2.0	-.50
.675	3.5	3.98	-.48	-1.5	-.38
.700	3.1	3.60	-.50	-1.5	-.38
.725	2.7	3.22	-.52	-2.0	-.50
.750	2.3	2.72	-.42	-1.0	-.25
.775	2.0	2.47	-.47	-1.5	-.38
.800	1.6	2.09	-.49	-1.5	-.38
.825	1.4	1.71	-.31	-0.8	-.20
.850	1.1	1.51	-.40	-0.9	-.22
.875	0.8	1.29	-.49	-1.5	-.38
.900	0.6	0.91	-.31	-0.8	-.20
.925	0.4	0.71	-.31	-0.8	-.20
.950	0.2	0.51	-.31	-0.8	-.20
.975	0.1	0.31	-.21	-0.5	-.12
1.000	0	0.19	****	****	****

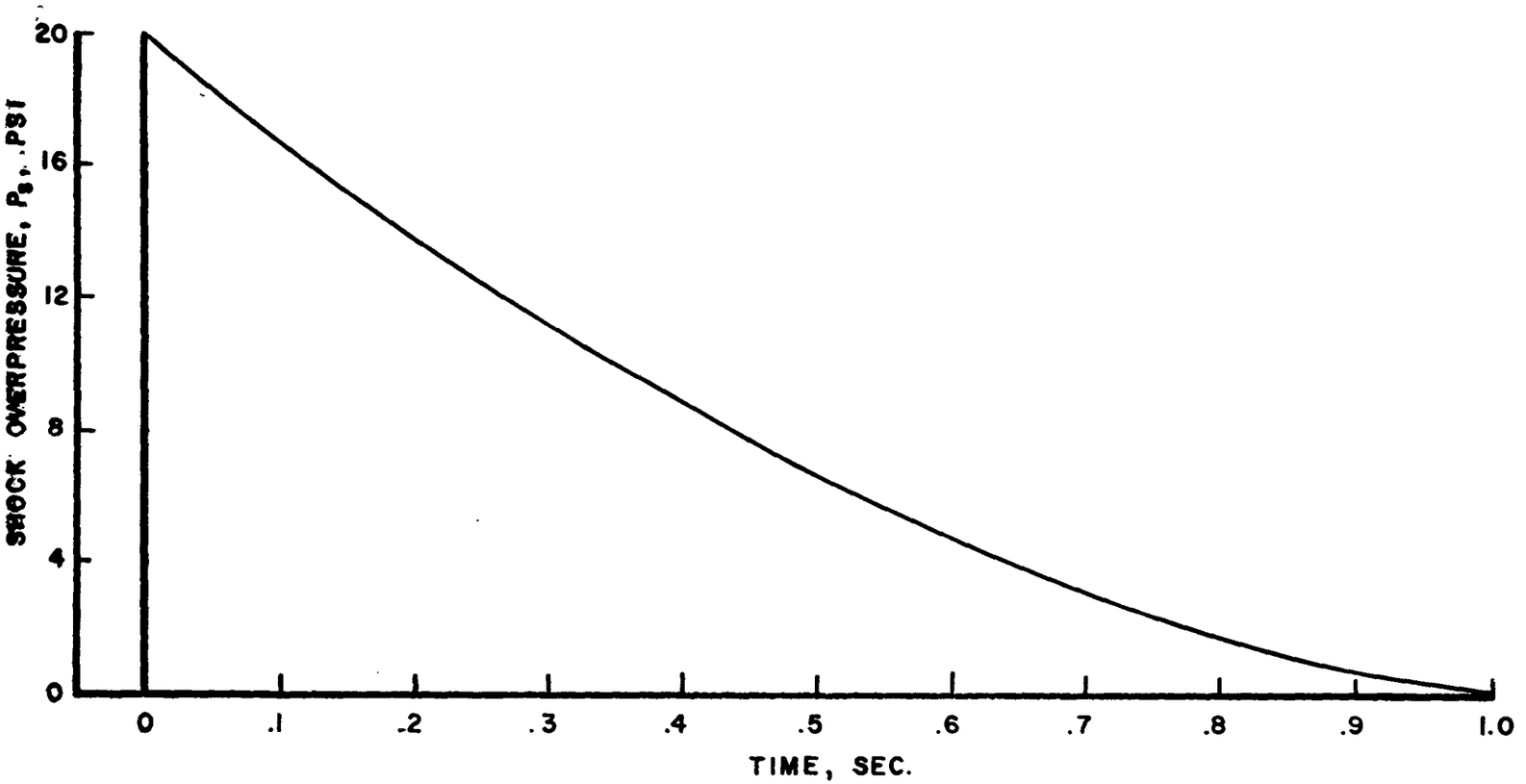

FIG. 7.4
APPLIED SHOCK WAVE

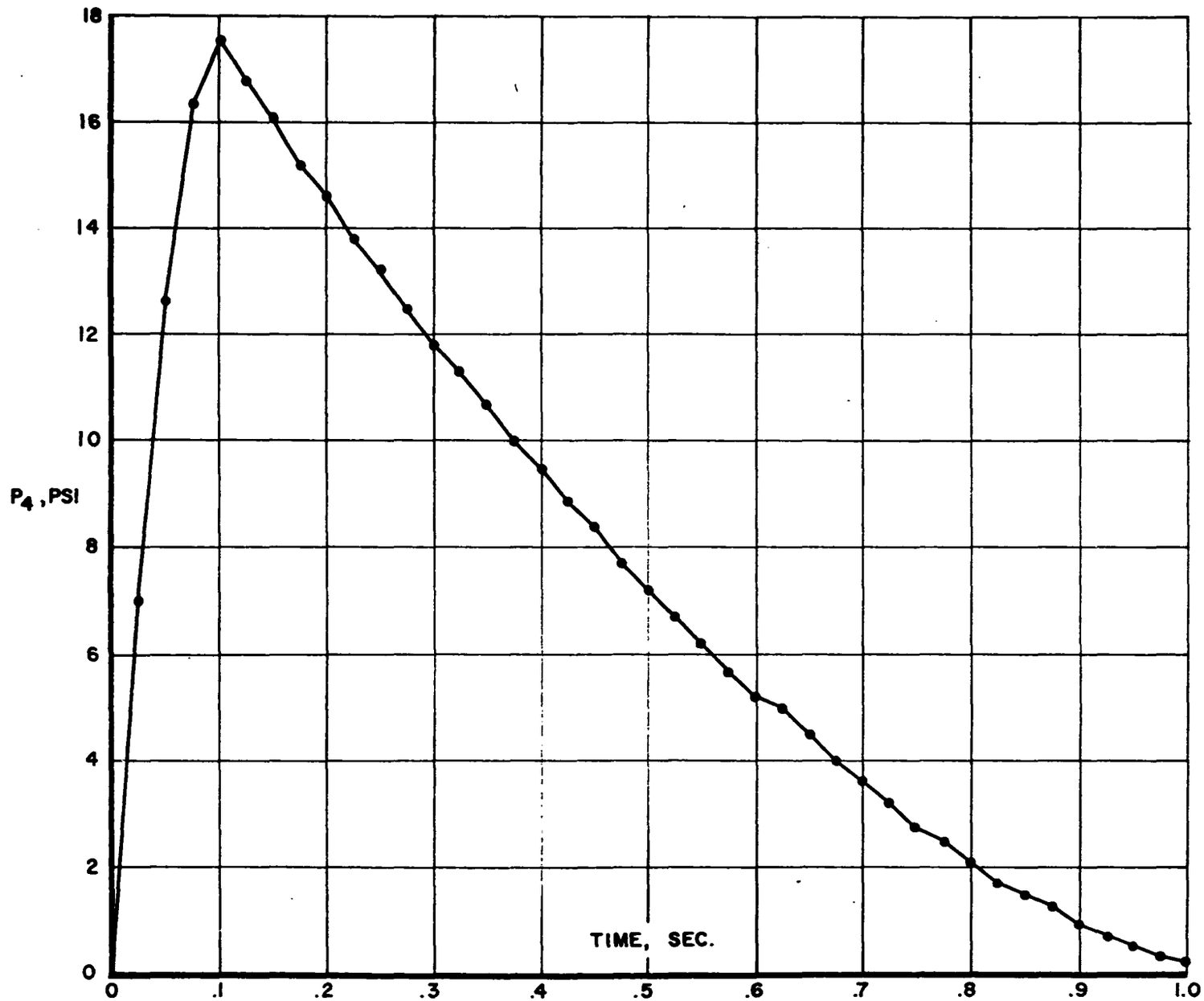

FIG. 7.5
CALCULATED PRESSURE-TIME HISTORY IN A CHAMBER

7.2 Tunnel Configurations With Chambers

The problem of shock waves applied to tunnel systems which lead to chambers has been studied with respect to the filling process of the chamber. It is shown in the previous section that if the wave shape at the entrance to the chamber is known, or can be predicted, the fill time curve in the chambers can be established. The pressure profile at the chamber entrance does not have to be the simple type discussed in Section 7.1.2 but may be complex as shown in Figure 7.1.

Figure 7.6 shows 3 tunnel systems which may be representative of existing designs. The single tunnel may be treated as a simple tunnel. Some notes on the other configurations are given in the following sections.

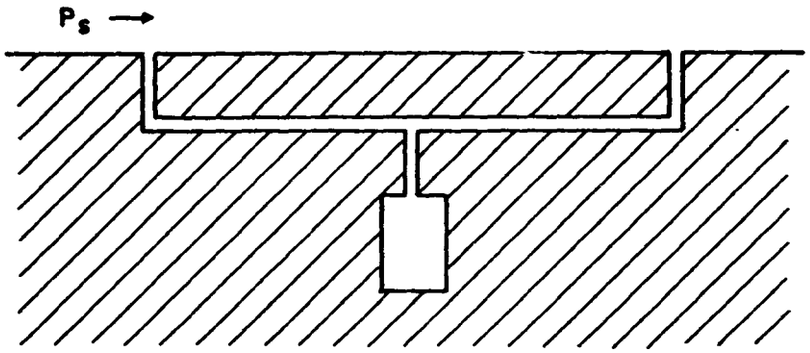

DOUBLE ENTRY TUNNEL

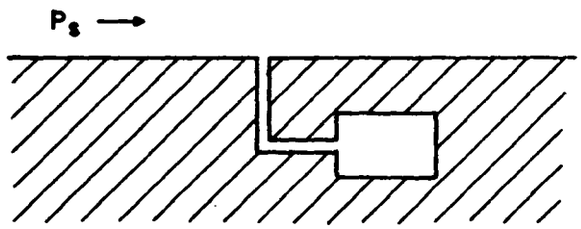

SINGLE TUNNEL

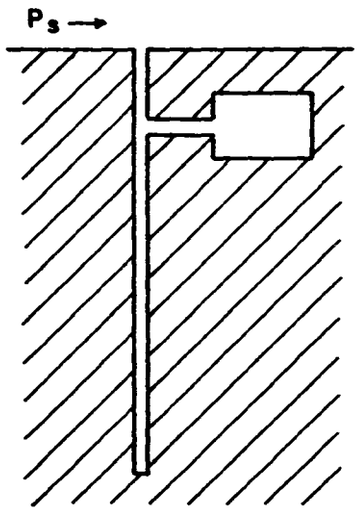

BY-PASS TUNNEL

FIG. 7.6
TUNNEL CHAMBER CONFIGURATIONS

7.2.1 The Multiple Entrance

In general the effect on the filling of a chamber by more than one tunnel will be similar to increasing the size of the one tunnel thereby causing a proportional increase in the rate of filling of the chamber. If two or more tunnels lead to a single inlet, the resulting fill rate will correspond to the enlarged entrance. It is concluded that the total tunnel entrance area should be a minimum in order to minimize the rate of pressure rise in the chamber.

7.2.2 The Bypass Entrance

The by-pass system, one that has a length of tunnel beyond the entrance, has the effect of reducing the rate of pressure rise in the chamber because it allows only part of the entrance flow to pass into the chamber. However, a by-pass should not be constructed for this purpose only, for the following reason.

For the by-pass to be effective it must be comparable in length to one-half the length of the shock wave entering the by-pass, otherwise the reflected pressures from the end of the by-pass will be applied to the chamber entrance. A study made of this length requirement showed that the volume of such a tunnel length should approach the volume of the chamber. If this tunnel volume is applied to the chamber, creating a larger volume, then the new rate of pressure rise in the chamber would be less than that created by the most efficient by-pass system. If the volume of the by-pass were made equal to the volume of the chamber and a simple configuration constructed with a new volume equal to the sum of the two, the reduction in fill rate of the larger chamber would be 25 percent greater than that accomplished by the chamber and by-pass system.

8. REFLECTED PRESSURES IN TUNNELS

When a shock wave impinges on a reflecting wall or blast resistant door, within a tunnel system, a reflected pressure is developed in the area of the wall or door. This reflected pressure sustains itself until it is relieved by a rarefaction from a low pressure area. The relief may come from another tunnel or chamber not yet full or from the entrance to the tunnel. When a shock wave is very long compared to the length of the tunnel, it is possible to have the entire tunnel under reflected pressure loading. Figure 2.2 shows the reflected pressure developed for corresponding values of applied pressure.

8.1 The Short Tunnel

A tunnel will be considered short if it is less than 10 diameters long. This limitation is established since experiments show that for distances less than 10 diameters the new shock in the tunnel is not fully developed.

8.1.1 The Short Tunnel Side-On

When a short tunnel is side-on to a blast, the resultant loading on a wall or door in the short tunnel becomes very complex. Figure 8.1a shows a sketch of such a configuration. In an extremely short tunnel, the blind end of the tunnel could be considered as the side wall of the tunnel. As this length is increased a diffraction pattern is set up on the walls (marked A and B in Figure 8.1a) and reflected pressures are developed. The pressure of the first reflection could be as high as the reflected pressure value for a shock wave in the main tunnel. The possibility of multiple reflections yielding still higher pressures exist. In addition to the reflections, stagnation pressure will be sustained in the region of wall B. The disadvantages of short tunnels or alcoves are therefore obvious. It should be mentioned however that the reflections that occur on wall A will be of relatively short duration and hence may not damage a door with a very long natural period of vibration.

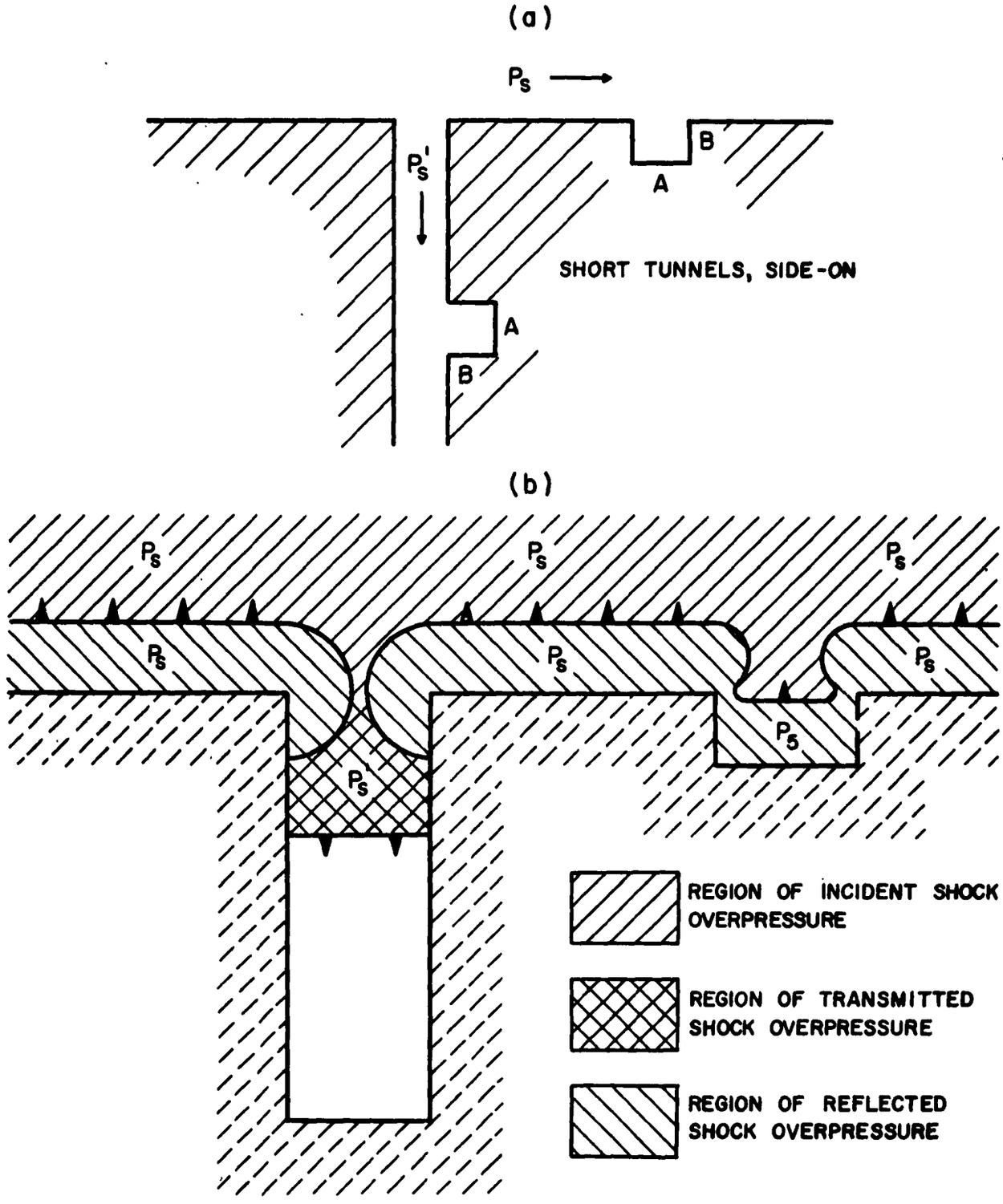

FIG. 8.1 - SHORT TUNNELS SIDE-ON AND FACE-ON

8.1.2 The Short Tunnel Face-On

A tunnel less than 10 diameters long and oriented face-on to the blast is considered short. Consider such a tunnel to have a large reflecting area about the tunnel entrance. In the limiting case, the tunnel will have no depth and the maximum pressure will be the pressure on the reflector (see Figure 8.1b). As the depth of the tunnel is increased the pressure in the tunnel increases in the reflected pressure. At a distance of 10 diameters in the tunnel the pressures will maximize. The maximum pressure on a reflecting wall is plotted in Figure 8.2 as a function of the applied pressure.

8.2 The Long Tunnel

The long, face-on, tunnel having a totally reflecting door or wall will sustain the reflected pressure plotted in Figure 8.2 if the blast wave did not attenuate. Under practical conditions the shock wave will not be infinitely long nor will the tunnel wall be smooth. Therefore, after the shock maximization the blast wave in the tunnel will begin to decay and the reflected pressure will be that associated with the new pressure value. For design purposes it would be wise to consider that the decay does not begin until the shock is 10 or more diameters down the tunnel. Blast wave attenuation is discussed in Chapter 5.

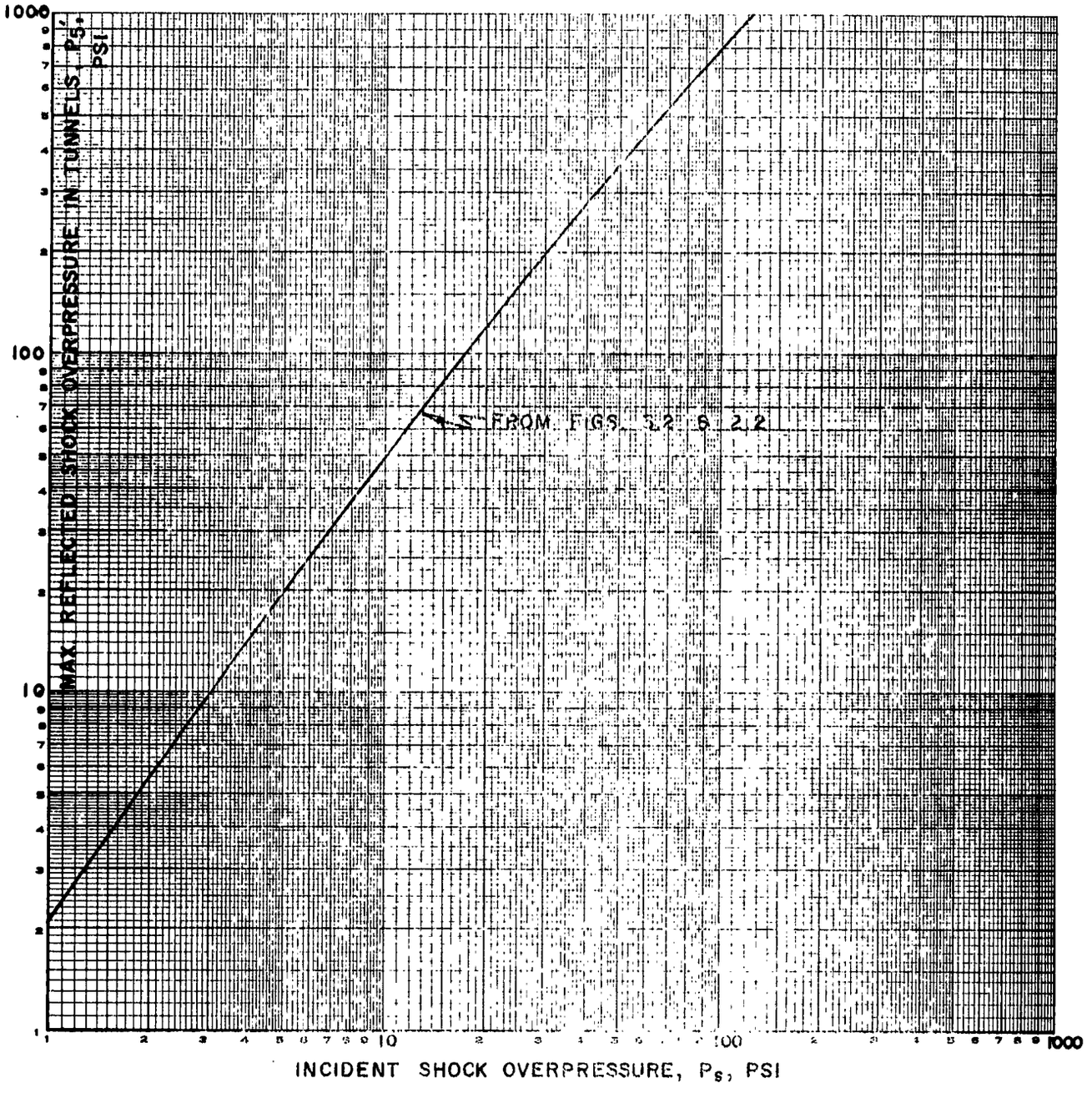

FIG. 8.2 – MAXIMUM REFLECTED SHOCK OVERPRESSURES IN SHORT FACE-ON TUNNELS AS A FUNCTION OF INCIDENT SHOCK OVERPRESSURES

8.3 Comparison of Reflected Pressures

Figure 8.3 shows plots of the reflected pressures developed in tunnels for three entrance conditions. The pressures are those that would be developed on reflecting walls or doors positioned at the shock maximization distances. The advantages of the side-on orientation is obvious.

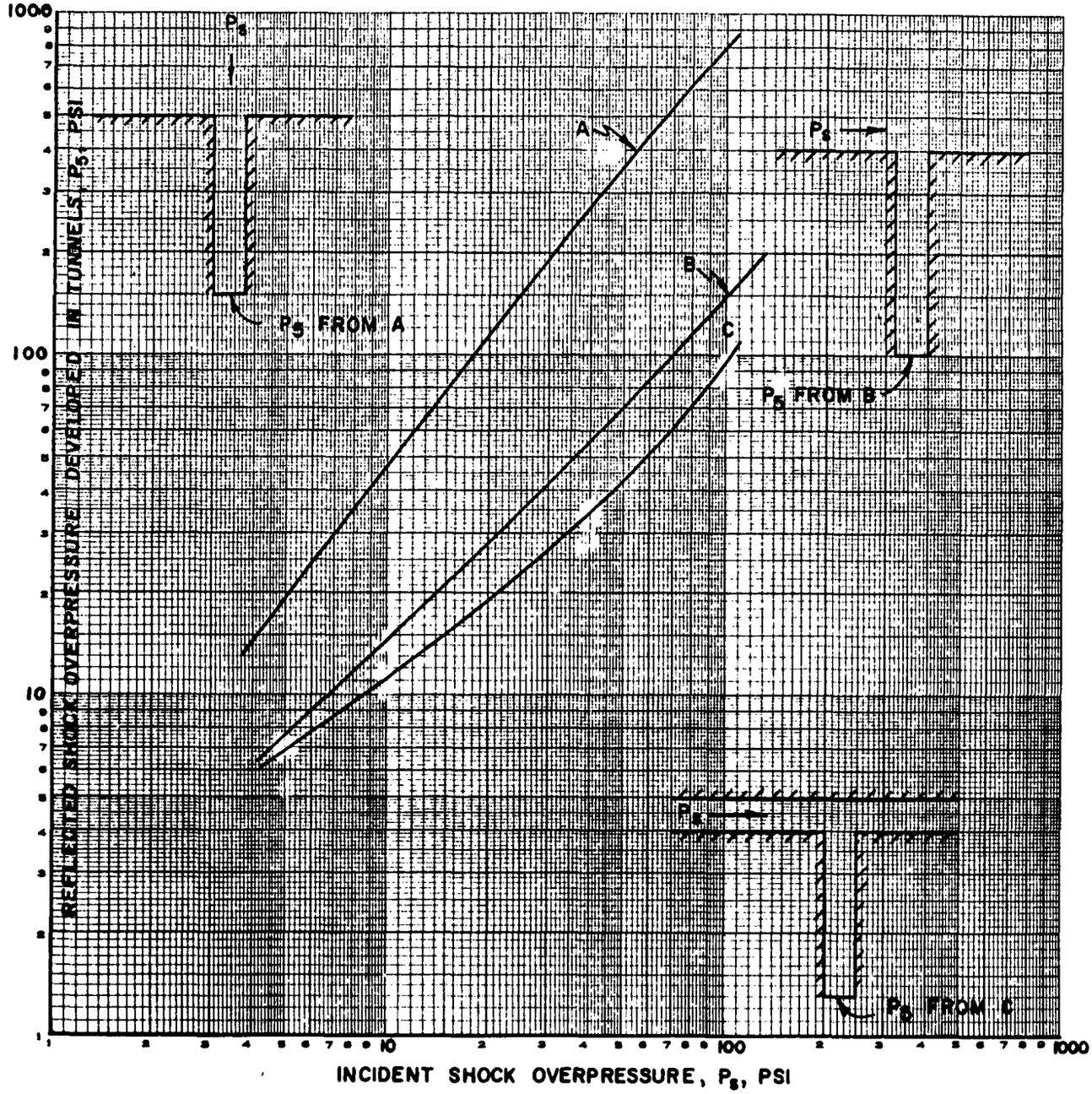

FIG. 8.3—REFLECTED SHOCK OVERPRESSURES DEVELOPED IN TUNNELS FOR THREE ENTRANCE CONDITIONS

9. BLAST ARRIVAL TIMES IN TUNNELS

9.1 Shock Front Arrival Time

Figure 2.1 is a plot of shock velocity as a function of shock overpressure and can be used for determining the blast arrival time in tunnels.

In approximating the arrival time between two stations in a straight uniform section of tunnel, the pressure is first predicted for the points under consideration, and the velocity of the wave at these points can be determined from Figure 2.1. The average velocity for the two points can be considered the velocity over the distance involved.

9.2 Time Interval Between Incident and Reflected Shock Waves in a Closed Tunnel

When a shock wave traveling down a tunnel reflects on a closed end of the tunnel, a reflected shock front is created and moves back into the original shock, causing a considerable increase in pressure. Section 3 of this report presents curves for determining maximum pressures in tunnels. In the event that certain of the tunnels have closed ends the pressures predicted (Section 3) are only the first shock pressures received. A second pressure, the reflected pressure will appear at a point in the tunnel at a time interval which is a function of the shock pressure, the ambient sound velocity, and the distance from the closed end to the point in question. The time required for a shock to pass a point in such a tunnel and for the reflection to return from the closed end is shown in Figure 9.1 for four different pressure levels.

The equations from which these curves are obtained are:

$$t = \frac{X}{U} + \frac{X}{U_5}$$

$$t = \frac{X}{a_o}\left[\frac{\left(1 + \frac{6P_o}{7P_s}\right)^{1/2}}{\left(\frac{2P_s}{7P_o} + 1\right)} + \frac{1}{\left(1 + \frac{6P_s}{7P_o}\right)^{1/2}}\right],$$

where X is the distance from the point in the tunnel to the closed end.

The equations are valid where loses, due to decay, in the distances are considered negligible and where the wave form is nearly constant over the times involved.

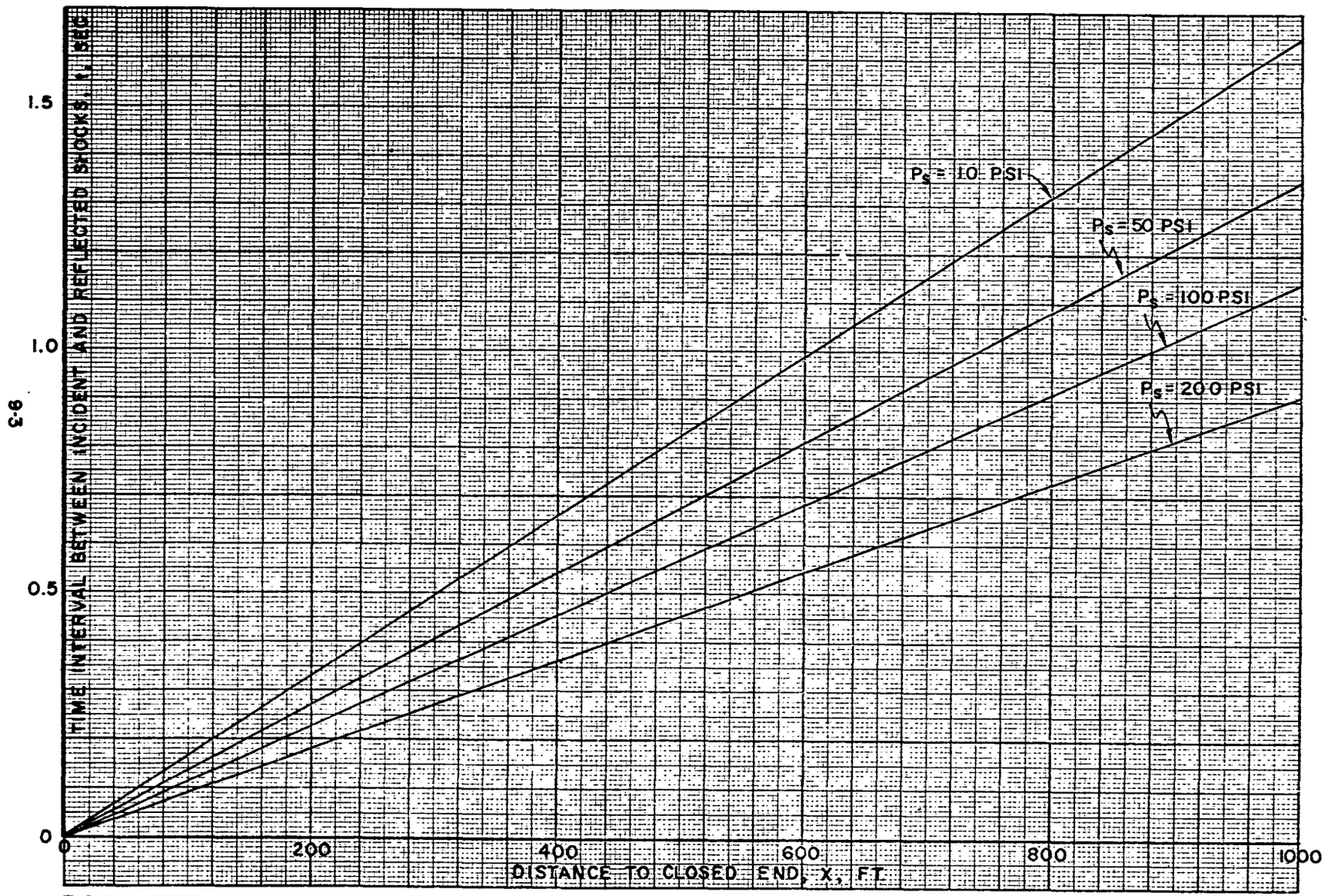

9-3

FIG. 9.1—TIME INTERVAL BETWEEN INCIDENT AND REFLECTED SHOCKS AS A FUNCTION OF DISTANCE & PRESSURE

DISTRIBUTION LIST

Organization	No. of Copies
Chief of Research and Development, DA, Washington 25, D. C., ATTN: Atomic Division	1
Chief of Ordnance, DA, Washington 25, D. C., ATTN: ORDTN ORDTB	2
Commanding General, U. S. Continental Army Command, Ft. Monroe, Virginia	1
President, U. S. Army Air Defense Board, Ft. Bliss, Texas	1
Commandant, U. S. Army Air Defense School, Ft. Bliss, Texas, ATTN: Command & Staff Department	1
Director, Special Weapons Development, Hq CONARC, Ft. Bliss, Texas, ATTN: Chester I. Peterson	1
Commanding General, U. S. Army Chemical Corps, R&D Command, Washington 25, D. C.	1
Commanding General, The Engineer Center, Ft. Belvoir, Virginia, ATTN: Commandant, Engineer School	1
Commanding Officer, Engineer Research & Development Lab., Ft. Belvoir, Virginia, ATTN: Chief, Tech Support Branch	1
Commanding Officer, Picatinny Arsenal, Dover, New Jersey, ATTN: ORDBB-TK	1
Commanding Officer, Transportation Research Command, Ft. Eustis, Virginia ATTN: Chief, Tech Info Div.	1
Commanding Officer, USA Signal R&D Lab, Ft. Monmouth, N. J., ATTN: Technical Documents Center, Evans Area	1
Commanding Officer, Chemical Warfare Lab., Army Chemical Center, Maryland, ATTN: Tech Library	1
Director, Waterways Experiment Station, P. O. Box 631, Vicksburg, Miss., ATTN: Library	1
Director, Operations Research Office, Johns Hopkins University, 6935 Arlington Road, Bethesda 14, Maryland	1
Chief of Engineers, Department of the Army, Washington, D. C. ATTN: ENGRD-NB ENGMC-EB ENGMC-DE	 3 10 3
Commanding General, The Engineer Center, Ft. Belvoir, Virginia, ATTN: Asst Commandant, Engineer School	1

Organization	No. of Copies
Commanding Officer, Engineer Research & Development Laboratory, Ft. Belvoir, Virginia, ATTN: Chief, Technical Support Branch	1
Director, Waterways Experiment Station, P. O. Box 631, Vicksburg, Mississippi, ATTN: Library	2
Corps of Engineers Ballistic Missile Construction Office, Air Force Unit Post Office, Los Angeles 45, California	1
U. S. Army Engineer Division, Mediterranean (Leghorn, Italy), APO 19, New York, New York	1
U. S. Army Engineer Division, Missouri River, P. O. Box 1216, Omaha, Nebraska	1
U. S. Army Engineer Division, New England, 424 Trapelo Road, Waltham 54, Massachusetts	1
U. S. Army Engineer Division, North Atlantic, 1216 Federal Office Building, 90 Church Street, New York 7, New York	1
U. S. Army Engineer Division, North Central, 536 South Clark Street, Chicago 5, Illinois	1
U. S. Army Engineer Division, North Pacific, 210 Custom House, Portland 9, Oregon	1
U. S. Army Engineer Division, Ohio River, 315 Main Street, P. O. Box 1159, Cincinnati, Ohio	1
U. S. Army Engineer Division, Pacific Ocean, Building 96, Fort Armstrong, Honolulu 13, Hawaii	1
U. S. Army Engineer Division, South Atlantic, P. O. Box 1889, Atlanta, Georgia	1
U. S. Army Engineer Division, South Pacific, 630 Sansome Street, Room 1216, San Francisco, California	1
U. S. Army Engineer Division, Southwestern, 1114 Commerce Street, Dallas 2, Texas	1
U. S. Army Engineer District, New York, 111 East 16th Street, New York 3, New York	1
U. S. Army Engineer District, P. O. Box 1715, Baltimore 3, Maryland	1
U. S. Army Engineer District, P. O. Box 119, Norfolk, Virginia	1
U. S. Army Engineer District, P. O. Box 4970, Jacksonville 1, Florida	1
U. S. Army Engineer District, P. O. Box 1169, Mobile, Alabama	1
U. S. Army Engineer District, P. O. Box 1600, Fort Worth, Texas	1

Organization	No. of Copies
U. S. Army Engineer District, P. O. Box 17277 Foy Station, Los Angeles, California	1
U. S. Army Engineer District, Omaha, 6012 U. S. Post Office & Court House, 215 No. 17th Street, Omaha 2, Nebraska	5
U. S. Army Engineer District, Albuquerque, P. O. Box 1538, Albuquerque, New Mexico	3
U. S. Army Engineer District, 1519 S. Alaskan Way, Seattle 4, Washington	3
U. S. Army Engineer District, Building 96, Fort Armstrong, Honolulu 13, Hawaii	3
Chief of Naval Operations, DN, Washington 25, D. C., ATTN: OP-75	2
OP-03EG	1
Director of Naval Intelligence, DN, Washington 25, D. C., ATTN: OP-922V	1
Chief, Bureau of Naval Weapons, DN, Washington 25, D. C.	2
Chief, Bureau of Ships, DN, Washington 25, D. C., ATTN: Code 372	1
Code 423	1
Chief, Bureau of Yards and Docks, DN, Washington 25, D. C., ATTN: D-400	1
D-440	1
Chief of Naval Research, DN, Washington 25, D. C., ATTN: Code 811	1
Commander-in-Chief, U. S. Pacific Fleet, FPO, San Francisco, California	1
Commander-in-Chief, U. S. Atlantic Fleet, U. S. Naval Base, Norfolk 11, Virginia	1
Commandant of the Marine Corps, DN, Washington 25, D. C., ATTN: Code A03H	4
President, U. S. Naval War College, Newport, Rhode Island	1
Superintendent, U. S. Naval Postgraduate School, Monterey, California	1
Commanding Officer, Nuclear Weapons Training Center, Atlantic, Naval Base, Norfolk 11, Virginia, ATTN: Nuclear Warfare Department	1
Commanding Officer, U. S. Naval Schools Command, U. S. Naval Station, Treasure Island, San Francisco, California	1
Commanding Officer, Nuclear Weapons Training Center, Pacific, Naval Station, North Island, San Diego 35, California	2
Commanding Officer, U. S. Naval Damage Control Training Center, Naval Base, Philadelphia 12, Pa., ATTN: ABC Defense Course	1

Organization		No. of Copies
Commander, U. S. Naval Ordnance Lab., White Oak, Silver Spring, Maryland	ATTN: EA	1
	EU	1
	E	1
Commander, U. S. Naval Ordnance Test Station, China Lake, California		1
Commanding Officer & Director, U. S. Naval Civil Engineering Laboratory, Port Hueneme, California, ATTN: Code L31		1
Director, U. S. Naval Research Laboratory, Washington 25, D. C.		1
Commanding Officer & Director, Naval Electronics Lab., San Diego 52, California		1
Commanding Officer, U. S. Naval Radiological Defense Laboratory, San Francisco, California, ATTN: Tech Info Division		1
Commanding Officer & Director, David W. Taylor Model Basin, Washington 7, D. C., ATTN: Library		1
Commander, Norfolk Naval Shipyard, Portsmouth, Virginia, ATTN: Underwater Explosions Research Division		1
Hq USAF (AFTAC) Washington 25, D. C.		1
Deputy Chief of Staff, Plans & Programs, Hq USAF, Washington 25, D. C., ATTN: War Plans Division		1
Director of Research & Development, DCS/D, Hq USAF, Washington 25, D. C., ATTN: Guidance & Weapons Division		1
Air Force Intelligence Center, Hq USAF, ACS/I (AFCIN-3V1), Washington 25, D. C.		1
Commander-in-Chief, Strategic Air Command, Offutt AFB, Nebraska, ATTN: OAWS		1
Commander, Tactical Air Command, Langley AFB, Virginia, ATTN: Document Security Branch		1
Commander, Air Material Command, Wright-Patterson AFB, Ohio		2
Commander, Air Research & Development Command, Andrews AFB, Washington 25, D. C., ATTN: RDRWA		1
Director, Air University Library, Maxwell AFB, Alabama		2
Commander, Wright Air Development Center, Wright-Patterson AFB, Ohio, ATTN: WCOSI		1
Commander, AF Cambridge Research Center, L. G. Hanscom Field, Bedford, Massachusetts, ATTN: CROST-2		1

Organization	No. of Copies
Commander, AF Special Weapons Center, Kirtland AFB, New Mexico, ATTN: Tech Info Office	1
Commandant, USAF Institute of Technology, Wright-Patterson AFB, Ohio, ATTN: MCLI-ITRIDL	1
Commander, Western Development Division (ARDC), P. O. Box 262, Inglewood, California	1
Director, USAF Project RAND, Via: U. S. Air Force Liaison Office, The RAND Corporation, 1700 Main Street, Santa Monica, California	1
Director of Civil Engineering, Hq USAF, Washington 25, D. C., ATTN: AFOCE	1
Director of Defense Research & Engineering, Washington 25, D. C., ATTN: Tech Library	1
U. S. Documents Officer, Office of the United States National Military Representative-SHAPE, APO 55, New York, N. Y.	1
Commander-in-Chief, Pacific, Fleet Post Office, San Francisco, Calif.	1
Director, Weapons Systems Evaluation Group, OSD, Room 1E880, The Pentagon, Washington 25, D. C.	1
Commandant, Armed Forces Staff College, Norfolk 11, Virginia, ATTN: Library	1
Commander, Field Command, DASA, Sandia Base, Albuquerque, New Mexico	2
Commander, Field Command, DASA, Sandia Base, Albuquerque, New Mexico, ATTN: Training Division	2
Chief, Defense Atomic Support Agency, Washington 25, D. C.	5
Chief, Defense Atomic Support Agency, Washington 25, D. C., ATTN: Major Vickery	2
Commandant, Army War College, Carlisle Barracks, Pa., ATTN: Library	1
Commandant, National War College, Washington 25, D. C., ATTN: Class Rec Library	1
Commandant, The Industrial College of the Armed Forces, Ft. McNair, Washington 25, D. C.	1
Officer-in-Charge, US Naval School, Civil Engineering Corps Officers, US Naval Construction Battalion, Port Hueneme, California	1
Los Alamos Scientific Laboratory, P. O. Box 1663, Los Alamos, New Mexico, ATTN: Report Librarian (For Dr. Alvin C. Graves)	1

Organization	No. of Copies
Administrator, National Aeronautics & Space Administration, 1512 "H" Street, NW, Washington 25, D. C.	1
Langley Research Center, NASA, Langley Field, Hampton, Virginia, ATTN: Mr. John Stack	1
Chief, Classified Technical Library, Technical Information Service, U. S. Atomic Energy Commission, Washington 25, D. C., ATTN: Mrs. Jean O'Leary (For Dr. Paul C. Fine)	1
Chief, Classified Technical Library, Tech Information Service, U. S. Atomic Energy Commission, Washington 25, D. C., ATTN: Mrs. Jean O'Leary	1
Dr. Walker Bleakney, Forestal Research Center Library, Aeronautical Sciences Building, Princeton University, Princeton, New Jersey, ATTN: Librarian	1
Manager, Albuquerque Operations Office, U. S. Atomic Energy Commission, P. O. Box 5400, Albuquerque, New Mexico	1
Dr. Robert J. Hansen, Division of Industrial Cooperation, Massachusetts Institute of Technology, 77 Massachusetts Ave., Cambridge, Massachusetts	1
Dr. Bruce G. Johnston, The University of Michigan, University Research Security Office, Lobby 1, East Engineering Bldg., Ann Arbor, Michigan	1
Sandia Corporation, Sandia Base, Albuquerque, New Mexico, ATTN: Classified Document Division (For M. L. Merritt)	1
Superintendent, Eastern Experiment Station, U. S. Bureau of Mines, College Park, Maryland, ATTN: Dr. Leonard Obert	1
Dr. Nathan M. Newmark, University of Illinois, Room 207, Talbot Lab., Urbana, Illinois	1
Commander, ASTIA, Arlington Hall Station, Arlington 12, Virginia, ATTN: TIPDR	20
Parsons, Brinkerhoff, Quade & Douglas, 165 Broadway, New York 6, New York, ATTN: Mr. S. Greenfield	2
Ammann & Whitney, 111 Eighth Avenue, New York, New York, ATTN: Mr. E. Cohen	2
Holmes & Narver Inc., AEC Facilities Division, 849 S. Broadway, Los Angeles 14, California, ATTN: Mr. Sherwood B. Smith	1

AD Accession No.
Ballistic Research Laboratories, APG
INFORMATION SUMMARY OF BLAST PATTERNS IN TUNNELS AND CHAMBERS (Second Edition)
Shock Tube Facility Staff

BRL Memorandum Report No. 1390 March 1962

OMSC No. 5010.21.83024
UNCLASSIFIED Report

UNCLASSIFIED

Shock tubes - Performance
Shock waves - Reflection
Shielding - Blast

The military requirements for protective construction have in recent years been most demanding since they include "blast hardened" designs. This in many cases means putting the construction deep underground and sets up requirements for information on the behavior of blast waves in confined region such as tunnels and chambers.

The Shock Tube Facility at the Ballistic Research Laboratories (BRL) endeavored to obtain information on the behavior of blast waves in tunnels and chambers by instrumenting models of simple tunnel configurations with piezo electric gages and subjecting the models to the blast wave from shock tubes. Data were obtained from models attached to the 24" circular tube, the 4" x 15" rectangular tube, and the high pressure tube. This report contains a compilation of the test results.

AD Accession No.
Ballistic Research Laboratories, APG
INFORMATION SUMMARY OF BLAST PATTERNS IN TUNNELS AND CHAMBERS (Second Edition)
Shock Tube Facility Staff

BRL Memorandum Report No. 1390 March 1962

OMSC No. 5010.21.83024
UNCLASSIFIED Report

UNCLASSIFIED

Shock tubes - Performance
Shock waves - Reflection
Shielding - Blast

The military requirements for protective construction have in recent years been most demanding since they include "blast hardened" designs. This in many cases means putting the construction deep underground and sets up requirements for information on the behavior of blast waves in confined region such as tunnels and chambers.

The Shock Tube Facility at the Ballistic Research Laboratories (BRL) endeavored to obtain information on the behavior of blast waves in tunnels and chambers by instrumenting models of simple tunnel configurations with piezo electric gages and subjecting the models to the blast wave from shock tubes. Data were obtained from models attached to the 24" circular tube, the 4" x 15" rectangular tube, and the high pressure tube. This report contains a compilation of the test results.

AD Accession No.
Ballistic Research Laboratories, APG
INFORMATION SUMMARY OF BLAST PATTERNS IN TUNNELS AND CHAMBERS (Second Edition)
Shock Tube Facility Staff

BRL Memorandum Report No. 1390 March 1962

OMSC No. 5010.21.83024
UNCLASSIFIED Report

UNCLASSIFIED

Shock tubes - Performance
Shock waves - Reflection
Shielding - Blast

The military requirements for protective construction have in recent years been most demanding since they include "blast hardened" designs. This in many cases means putting the construction deep underground and sets up requirements for information on the behavior of blast waves in confined region such as tunnels and chambers.

The Shock Tube Facility at the Ballistic Research Laboratories (BRL) endeavored to obtain information on the behavior of blast waves in tunnels and chambers by instrumenting models of simple tunnel configurations with piezo electric gages and subjecting the models to the blast wave from shock tubes. Data were obtained from models attached to the 24" circular tube, the 4" x 15" rectangular tube, and the high pressure tube. This report contains a compilation of the test results.

AD Accession No.
Ballistic Research Laboratories, APG
INFORMATION SUMMARY OF BLAST PATTERNS IN TUNNELS AND CHAMBERS (Second Edition)
Shock Tube Facility Staff

BRL Memorandum Report No. 1390 March 1962

OMSC No. 5010.21.83024
UNCLASSIFIED Report

UNCLASSIFIED

Shock tubes - Performance
Shock waves - Reflection
Shielding - Blast

The military requirements for protective construction have in recent years been most demanding since they include "blast hardened" designs. This in many cases means putting the construction deep underground and sets up requirements for information on the behavior of blast waves in confined region such as tunnels and chambers.

The Shock Tube Facility at the Ballistic Research Laboratories (BRL) endeavored to obtain information on the behavior of blast waves in tunnels and chambers by instrumenting models of simple tunnel configurations with piezo electric gages and subjecting the models to the blast wave from shock tubes. Data were obtained from models attached to the 24" circular tube, the 4" x 15" rectangular tube, and the high pressure tube. This report contains a compilation of the test results.